

Sorption properties of Eu onto granite
and MX-80 bentonite in Ca-Na-Cl
solutions

SORPTION PROPERTIES OF EU ONTO GRANITE AND
MX-80 BENTONITE IN CA-NA-CL SOLUTIONS

By

JIANAN LIU, B.A.Sc.

A THESIS

SUBMITTED TO THE DEPARTMENT OF ENGINEERING PHYSICS

AND THE SCHOOL OF GRADUATE STUDIES

OF MCMASTER UNIVERSITY

IN PARTIAL FULFILLMENT OF THE REQUIREMENTS

FOR THE DEGREE OF

MASTER OF APPLIED SCIENCE

© Copyright by Jianan Liu, July 2023

Master of Applied Science (2023)

McMaster University

(Engineering Physics)

Hamilton, Ontario, Canada

TITLE: Sorption properties of Eu onto granite and MX-80
bentonite in Ca-Na-Cl solutions

AUTHOR: Jianan Liu
B.A.Sc. (Engineering Physics)
Queen's University, Kingston, Ontario, Canada

SUPERVISOR: Dr. Shinya Nagasaki

NUMBER OF PAGES: xiv, 72

For all those who supported me throughout my study

Abstract

Plutonium (Pu) is one of the key elements in high-level radioactive waste due to its long half-life. Understanding the sorption behavior of key radionuclides such as Pu and U is important to the safety assessment calculation for a deep geological repository for high-level radioactive waste. Europium (III) (Eu(III)), a chemical analogue of Pu, has shared similar sorption behaviors as Pu. The aim of this study is to investigate the sorption properties of europium onto MX-80 bentonite and crystalline rock (granite), a potential host rock for a deep geological repository for some countries, as a function of pH and ionic strength using batch experiment technique and surface complexation modeling. The experiments are conducted in Ca-Na-Cl solutions. For granite, the sorption coefficient K_d showed proportionate dependence on the pH. The sorption of Eu is dependent on ionic strength at near neutral to low pH region while not dependent on ionic strength at higher pH. For MX-80 bentonite, the sorption of Eu has little dependence on the ionic strength. A surface complexation modeling is also being carried out to examine the experimental results and identify the possible mechanism of the sorption.

Contents

Abstract	iv
Acknowledgement	xii
Abbreviations	xiii
Nomenclatures	xiv
1. Introduction.....	1
1.1 Background	1
1.2 Literature review	4
1.2.1 Review of sorption experiments	4
1.2.2 Review of modeling	7
1.3 Purpose	8
2. Theory.....	9
2.1 Sorption mechanism.....	9
2.1.1 Non-specific sorption.....	9
2.1.2 Specific sorption	13
2.2 Experiment setup.....	15
2.3 Sorption modelling.....	16
2.3.1 Surface complexation reactions modeling	17

2.3.2	Ionic exchange reactions	18
3	Experimental Methods	19
3.1	Materials & Equipment	19
3.2	Preparation of solutions.....	19
3.3	Detection limit of Eu (III)	20
3.4	Eu (III) Solubility	21
3.5	Eu (III) Kinetics	21
3.6	pH and ionic strength dependence of Eu (III) sorption	22
4	Sorption modeling	24
4.1	Thermodynamic data.....	24
4.2	Surface definition	26
4.3	Surface complexation reaction & Ionic exchange reactions	28
5	Results and Discussion	30
5.1	Solubility	30
5.2	pH dependence and ionic strength dependence of Eu (III) sorption	31
5.3	PHREEQC modeling.....	40
5.3.1	Modeling results for Eu sorption onto granite	44
5.3.2	Modeling results for Eu sorption onto MX-80 bentonite.....	53
6	Future work.....	63
7	Conclusion	64
8	Bibliography	66

List of Tables

Table 1: The salt masses of Ca-Na-Cl solutions for each ionic strength	20
Table 2: The ion concentration of Ca-Na-Cl solutions for each concentration.....	24
Table 3: Formation reactions and associated constants of the relevant species from JAEA database (Kitamura et al., 2014) and (Spahiu & Bruno, 1995).....	25
Table 4: SIT parameters for the species in this modeling (Kitamura et al., 2014).....	26
Table 5: Defined surface site in the modeling for granite. “_sOH” stands for strong site while “w_OH” stands for weak site. “Surf_xNa” represents the ionic exchange site (Iida et al., 2016).	27
Table 6: Defined surface site in the modeling for MX80-bentonite. “_sOH” stands for strong site while “w_OH” stands for weak site. “ww_OH” stands for the second weak site considered in the model. “Surf_xNa” represents the ionic exchange site (Grambow et al., 2006).	28
Table 7: The protonation and deprotonation reactions for the components of granite (Iida et al., 2016).	29
Table 8: The protonation and deprotonation reactions with associated constants for the montmorillonite (Bradbury & Baeyens, 2005).	29

Table 9: The surface complexation and ionic exchange reactions with their constants from the optimized model.....	52
Table 10: The main reactions identified for the sorption of Eu onto granite.	53
Table 11: The surface complexation and ionic exchange reactions with their constants from the optimized model.	60
Table 12: The hydrolysis constants ($\log OHKx$) for related aqueous species referenced from JAEA database (Kitamura et al., 2014).	61

List of Figures

Figure 1: The schematic for the conceptual design of deep geological repository (Naserifard et al., 2021).	2
Figure 2: The existence form of the surface site over pH 0-12 (Stumm, 1995).	11
Figure 3: The schematic of Stern layer (Stern, 1924).	12
Figure 4: The pH dependence of the binding of metal ions (Stumm, 1995).....	13
Figure 5: Schematic of Surface complex formation. “s” stands for the surface hydroxyl group, “a” represents inner-sphere complexes, “β” is outer-sphere complexes, and “d” is diffusion ion swarm (Stumm, 1995).	14
Figure 6: The schematic of batch sorption experiment method (Riddoch, 2016).....	15
Figure 7: Solubility of Eu in 0.05 m and 1 m Ca-Na-Cl solutions over a 21-day period. .	31
Figure 8: Experimental results for sorption of Eu onto granite.	32
Figure 9: Experimental results for sorption of Eu onto MX-80 bentonite.....	33
Figure 10: The sorption coefficient value K_d for Eu sorption onto granite as a function of ionic strength at around pH4 and pH5.	34
Figure 11: The sorption coefficient value K_d for Eu sorption onto granite as a function of ionic strength at around pH8-9.	35
Figure 12: The sorption coefficient value K_d for Eu sorption onto MX-80 bentonite as a function of ionic strength at around pH6,7,8.	36

Figure 13: Comparison of sorption results onto granite with previous work. The solution type of other work include 0.1M NaCl solution and 0.033M CaCl₂ solution in (Jin et al., 2014), and 0.1M NaCl solution in (Fukushi et al., 2013), “M” stands for molarity (mol/L), “m” is molality (mol/kg)..... 39

Figure 14: Comparison of sorption results onto MX-80 bentonite with other work. The solution type for other work is 0.066M Ca(NO₃)₂ in (Bradbury & Baeyens, 2002) and (Fernandes et al., 2008), 0.066M Ca(ClO₄)₂ in (Rabung et al., 2005), and 0.1M NaCl in (Z. Guo et al., 2009), “M” stands for molarity (mol/L), “m” is molality (mol/kg). 39

Figure 15: The solution speciation of Eu in Ca-Na-Cl solution. (a) is in 1 m solution, (b) is in 0.5 m solution, (c) is in 0.24 m solution, (d) is in 0.1 m solution, and (e) is in 0.05 m solution..... 43

Figure 16: The sorption modeling for the sorption of Eu onto granite at 1 m Ca-Na-Cl solution. (a) is the speciation of surface complex; (b) is the curve fitting for the experimental results. 45

Figure 17: The sorption modeling for the sorption of Eu onto granite at 0.5 m Ca-Na-Cl solution. (a) is the speciation of the surface complex; (b) is the curve fitting for the experimental results. 46

Figure 18: The sorption modeling for the sorption of Eu onto granite at 0.24 m Ca-Na-Cl solution. (a) is the speciation of the surface complex; (b) is the curve fitting for the experimental results. 47

Figure 19: The sorption modeling for the sorption of Eu onto granite at 0.1 m Ca-Na-Cl solution. (a) is the speciation of the surface complex; (b) is the curve fitting for the experimental results.	48
Figure 20: The sorption modeling for the sorption of Eu onto granite at 0.05 m Ca-Na-Cl solution. (a) is the speciation of the surface complex; (b) is the curve fitting for the experimental results.	49
Figure 21: The sorption modeling for the sorption of Eu onto MX-80 bentonite in 1 m Ca-Na-Cl solution. (a) is the speciation of the surface complex; (b) is the curve fitting for the experimental results.	54
Figure 22: The sorption modeling for the sorption of Eu onto MX-80 bentonite in 0.5 m Ca-Na-Cl solution. (a) is the speciation of the surface complex; (b) is the curve fitting for the experimental results.	55
Figure 23: The sorption modeling for the sorption of Eu onto MX-80 bentonite in 0.24 m Ca-Na-Cl solution. (a) is the speciation of the surface complex; (b) is the curve fitting for the experimental results.	56
Figure 24: The sorption modeling for the sorption of Eu onto MX-80 bentonite in 0.1 m Ca-Na-Cl solution. (a) is the speciation of the surface complex; (b) is the curve fitting for the experimental results.	57
Figure 25: The sorption modeling for the sorption of Eu onto MX-80 bentonite in 0.05 m Ca-Na-Cl solution. (a) is the speciation of the surface complex; (b) is the curve fitting for the experimental results.	58

Acknowledgement

I would like to thank my supervisor, Dr. Shinya Nagasaki, for all his guidance and help throughout my study at McMaster University. I also would like to thank my colleagues, Dr. Fabiola Guido, Dr. Zhiwei Zheng, Joshua Racette, and Jieci Yang, for all their helpful discussion and support with conducting the experiments and modeling. I would like to thank Dr. Tammy Yang from the NWMO for all the reviews and comments on my work and reports. Finally, I would like to thank all my family and friends for their support and encouragement throughout my study.

This work is funded by the Nuclear Waste Management Organization.

Abbreviations

APM	Adaptive Phased Management
CA	Component Additivity
CPS	Count per second
DGR	Deep geologic repository
DI	Deionized water
GC	General Composite
ICPMS	Inductively coupled plasma mass spectrometry
JAEA	Japan atomic energy agency
NWMO	Nuclear Waste Management Organization
PHREEQC	PH Redox Equilibrium in C
SIT	Specific Ion Theory
SSA	Specific surface area
TDB	Thermodynamic database
TRLFS	Time-resolved Laser Fluorescence Spectroscopy
UFC	Used-fuel container
XPS	X-ray electron spectroscopy

Nomenclatures

C_{eq}	the concentration of the ion in solution at equilibrium
C_i	the initial concentration of the ion in solution
L	volume of liquid
K_d	sorption coefficient value
I	ionic strength
M	Molarity
m	Molality

1. Introduction

1.1 Background

The nuclear energy has experienced exponential growth and development since it was introduced as an energy provider. It also plays a crucial role in achieving neutral carbon economy. The nuclear waste, however, is a by-product from the nuclear reactors and is considered as a health risk due to its high radioactivity and toxicity. As of June 30, 2022, the amount of used nuclear fuel bundles were about 3.2 million in Canada, and it could be added up to about 5.5 million bundles if all existing reactors are to be operated to their full lifespan (Naserifard et al., 2021). Presently, the used nuclear fuel bundles are placed in a water-filled pool for seven to ten years to cool their heat and reduce their radioactivity, followed by being transported to a dry storage facility. The radioactive elements in the used nuclear fuel such as uranium (U) and plutonium (Pu) will remain a health risk for many hundreds of thousands of years. For this reason, a careful long-term management of the used nuclear fuel is needed.

Nuclear Waste Management Organization (NWMO) is responsible for the safe and long-term management of Canada's used nuclear fuel. The approach is to safely contain and isolate the used nuclear fuel in a deep geological repository (DGR) in a suitable host rock formation. DGR has been internationally recognized and accepted as a solution to the nuclear spent fuel, with which many countries have selected as the technical method

to deal with their nuclear waste. For example, the construction of a DGR has already been underway in Finland. Figure 1 shows a conceptual design of the deep geological repository in Canada (Naserifard et al., 2021). The DGR is a multiple barrier system, including the nuclear fuel pellet, the used fuel bundle, the used fuel container, bentonite clay, and the geosphere (Naserifard et al., 2021).

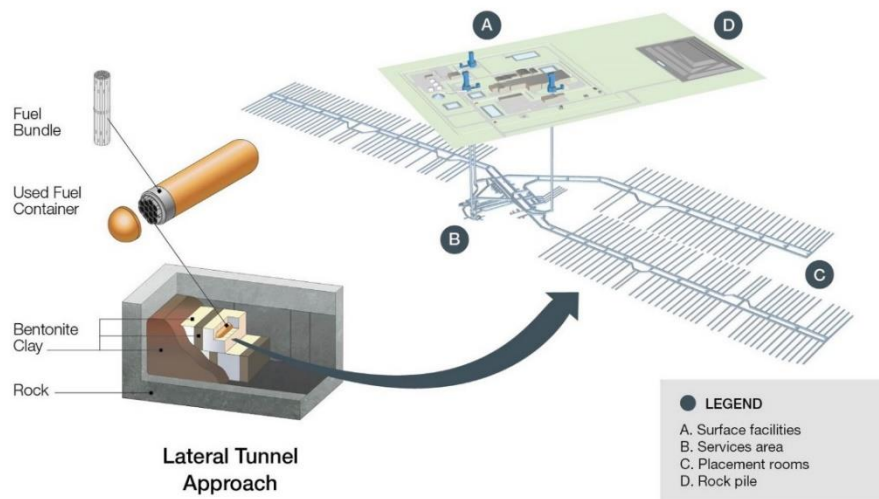


Figure 1: The schematic for the conceptual design of the deep geological repository (Naserifard et al., 2021).

Currently, both sedimentary rock and crystalline rock are being considered as potential host rock for a DGR in Canada. Bentonite will be used as the backfill material as well as the material for encasement of the used fuel containers in the repository.

The used fuel container is designed to last for tens of millions of years. However, as the radioactivity of the used nuclear fuel will last a very long period of time, the safety assessment will address various scenarios including scenarios that the used fuel container is compromised, followed which radionuclides are released to the engineered barrier

system. The bentonite clay in the engineered barrier system and the host rock in the geosphere will retard the radionuclides from the repository to reach the environment.

Plutonium (Pu) is one of the elements of interest to the safety assessment and is included in the NWMO sorption data report (Vilks & Yang, 2018). The main oxidation states of Pu include Pu (III), Pu (IV), Pu (V), and Pu (VI), among which Pu (III) are expected to be dominant under reducing conditions that are expected at the depth of the repository (Vilks & Yang, 2018). However, the plutonium is hard to use in the university.

Europium (Eu), a chemical analogue to plutonium, has been widely used to study and predict the sorption behavior of trivalent actinides such as Plutonium (Pu), Americium (Am), and Curium (Cm) (Bradbury & Baeyens, 2002) (Z. Guo et al., 2009) (Ortiz-Oliveros et al., 2021). (Lee et al., 2006) studied the sorption behavior of Eu and Am onto various geological materials using batch experiment method. The results showed that Eu shares similar sorption behaviour on these geological materials with Am and suggested that Eu could be used as an analogue of Am in geological structures, despite of pH variation.

This thesis will study the sorption properties of Eu onto granite and MX-80 bentonite in Ca-Na-Cl solution which have been observed in the Canadian crystalline rocks at depths of the repository.

1.2 Literature review

1.2.1 Review of sorption experiments

Granite is a crystalline rock being considered as the potential host rock for a DGR (e.g. by Sweden, Finland, Canada, Japan). Its major constituents include feldspar, quartz, and biotite. The sorption of radionuclides on granite and on its main components has been studied in the context of DGR, including sorption of Eu, Am, and Cm. The main focuses of the studies include the effect of pH, ionic strength, temperature, and organic/inorganic ligands on sorption. The sorption mechanisms have also been studied by surface complexation modeling and mineral/structure analysis. (Fukushi et al., 2013) found that the main sorption affinity of Eu sorption onto granite could be biotite and a single-site cation exchange reaction was able to reasonably explain the sorption at the neutral to acidic pH region (pH 2 - 6). (Jin et al., 2014) observed that the sorption of Eu and Am onto Beishan granite in 0.1M NaCl solution has strong dependence on pH while is independent of temperature at 25-80 °C. It was also found that biotite was the main contributor of the sorption and the presence of fulvic acid could significantly affect the sorption of Eu at pH > 4. (Karimzadeh et al., 2020) observed the negative effects of organic acid on the sorption of Eu (III) onto quartz using batch experiment. (Bezzina et al., 2022) quantified the pH dependence of the sorption experiments of Am, Cm, and Eu, and identified two inner-sphere complex species by using time-resolved laser fluorescence spectroscopy (TRLFS) results on Cm. (P. Li, Wu, et al., 2017) found the sorption of Eu onto K-feldspar is strongly dependent on pH and is mainly dominant by

outer-sphere complexes and inner-sphere complexes. (Neumann et al., 2021) conducted a comprehensive study of the sorption of Eu, Am, and Cm on K-feldspar.

Bentonite is considered as a potential material for the encasement of the fuel bundle and backfill material in the repository, due to its high sorption capacity and low permeability. Several studies were conducted to examine its ability to retard the radionuclides with related factors and possible mechanisms. (Z. Guo et al., 2009) studied the effects of CO₂ on sorption of Eu onto Na-bentonite using batch experiment technique. (N. Guo et al., 2015) extensively examined the effects of organic acids on the sorption of Eu onto Na-bentonite and found that the concentration ratio of Eu (III) to the organic ligand plays a key factor on the sorption. It was also found that the sorption of Eu on Na-bentonite increases with the pH increasing. (He et al., 2020) studied the impacts of pH, contact time, and temperature on Eu sorption onto MX-80 bentonite and observed that the temperature has a negative effect on the sorption. The main component of the bentonite is montmorillonite. (Rabung et al., 2005) studied the sorption of Eu and Cm onto Ca-montmorillonite and Na-illite. It was found that the outer-sphere complex was not formed on Ca-montmorillonite as much as that on Na-illite, since Ca²⁺ competes with the traced element on the cation-exchange site. (Sheng et al., 2009) observed an inverse relation between the ionic strength and sorption at pH = 2.50, and pH has a significant impact on the sorption of Eu onto montmorillonite. (Wang et al., 2015) examined the sorption mechanism of Eu sorption onto MX-80 bentonite and identified the point of complex change from outer-sphere complex to inner-sphere complex using TRLFS.

The sorption of Eu on other minerals such as kaolinite and calcite were also studied. For example, (Tertre et al., 2006) examined the effects of temperature on the sorption of Eu onto kaolinite and montmorillonite in NaClO₄ solution. It identified a unique inner-sphere sorption complex related to aluminol sites and found that higher temperature leads the sorption shifts to lower pH region. (Zavarin et al., 2005) studied the sorption of Eu(III) on calcite. (Zhang et al., 2021) studied the sorption of Eu onto Tamusu clay under high ionic strength (0.06M – 0.6M) and found that the sorption of Eu decreased as the ionic strength increased.

Additionally, there are research works studying the sorption of Eu onto metal oxides. (Qi et al., 2015) studied the adsorption of Eu(III) on FeNi/NGO composites and examined the effects of pH, ionic strength, and humic acid. (Tan et al., 2009) researched the sorption of Eu(III) onto TiO₂ and utilized X-ray electron spectroscopy (XPS) analysis to examine the chemical existence of Eu at the near-surface of TiO₂. (Kumar et al., 2013) presented the speciation of Am(III)/Eu(III) sorption on gamma-alumina and studied the effects of ion concentration on the sorption at low ionic strength (0.005-0.1M NaClO₄). (Fan et al., 2014) observed the sorption edge of Eu onto γ -Al₂O₃ shifted towards high pH as the concentration of Eu increased.

As there were many previous studies investigating the sorption properties of Eu, however, the solution condition of most studies is NaCl or NaClO₄ solutions with relatively low ionic strength – mostly ranging from 0.01M to 0.1M. Few studies systematically investigated the effects of pH and ionic strength over a wide range and in

saline conditions – particularly in Ca-Na-Cl solutions, which is also the groundwater condition of a potential DGR hosting site.

1.2.2 Review of modeling

The sorption modeling helps elucidate possible sorption mechanism by fitting with the experimental data, and examine the surface complexes of the sorption, thus gained interest of many studies. (Bradbury & Baeyens, 2002) utilized the sorption of Eu onto montmorillonite to test the applicability of a sorption model developed for the interpretation of the sorption mechanism for trivalent elements. (Hurel & Marmier, 2010) compared the component additivity (CA) approach with the general composite (GC) approach on the sorption of Eu onto MX-80 bentonite. It was found that the CA is capable of well reproducing the experimental data from pH 5.5 to 7.5. (Jin et al., 2014) carried out a GC model that successfully described the sorption of Eu on granite using PHREEQC. (Z. Guo et al., 2009) was able to describe the sorption of Eu onto Na-bentonite using a double layer model in the PHREEQC code.

However, most studies considered the mineral as a single surface site, using the general composite (GC) approach, to describe the sorption data. For minerals with complex assemblages such as granite, there is few research conducted that examined the effects of each component on Eu sorption and their sorption affinity, as this information may provide further understanding on the sorption mechanism.

1.3 Purpose

The purpose of this study is to investigate the sorption properties of Eu (III) onto granite and MX-80 bentonite in Ca-Na-Cl solutions, under saline and reducing conditions. The studied pH ranges from 4-9 and the ionic strength of the solution includes 0.05 m, 0.1 m, 0.24 m, 0.5 m, and 1 m, as expected conditions at the DGR site. The measured K_d values over a wide range of pH and ionic strengths can be used for the safety assessment calculation for a deep geological repository for used nuclear fuel. Also, this work aims to explore sorption mechanism and identify the possible complex species formed in the process using modeling method. Particularly, the modeling utilized the component additivity (CA) approach that helps identify the sorption distribution on the main components of granite. The modeling for Eu sorption onto MX-80 is also being carried out to help interpret the sorption mechanism.

2. Theory

This chapter outlines the theory and principles involved in this work, including the basic sorption mechanism, the experiment approach, and the modeling.

2.1 Sorption mechanism

According to (Stumm, 1995), adsorption is described as “accumulation of matter at the solid-water interface” and is “the basis of many surface-chemical process”. While sorption is a more general term that describes the process that a chemical is associated with solid phases.

Sorption can involve various mechanisms, largely determined by properties such as the chemical composition of the aqueous solutions and the surface sorption site. The main mechanisms considered in this work are non-specific sorption and specific chemical sorption.

2.1.1 Non-specific sorption

The non-specific sorption, also known as non-specific Columbic sorption, mainly involves processes caused by Columbic force. Mineral surfaces may contain surface charges caused by the permanent structural charge, coordinative surface charge, or dissociated surface charge (Davis & Kent, 2018). The permanent structural charge of a

mineral surface can usually be caused by an isomorphous substitution in the mineral. For instance, small quantities of Si^{4+} are replaced by Al^{3+} in a tetrahedral layer, thus leading to a negatively charged structure. Similarly, Al^{3+} can be replaced by Mg^{2+} in an octahedral layer, which leads to a negative charge imbalance in the structure (Stumm, 1995). Also, the surface charge can be resulted from the chemical reactions occurred at the surface sites. Under the interruption of the gibbsite and silica sheet, the crystal edges of the surface may contain broken bonds (Stumm, 1995). Since metal ions in the surface layer have a reduced coordination number, they behave as Lewis acid (Stumm, 1995). Under the presence of water, these metal ions share a tendency to coordinate with the water molecules, thus a neutral surface will be formed, as shown in equation (2.1),



The surface site can then go through protonation or deprotonation to form a positively charged surface or a negatively charged surface, as expressed in equations (2.2) and (2.3),



The protolysis equilibrium constants of these reactions are intrinsic to the corresponding surface sites and minerals. Figure 2 presents an example of the dominating species in the surface site as a function of pH. The dominating charge of the surface sites is positive at low pH and negative at high pH.

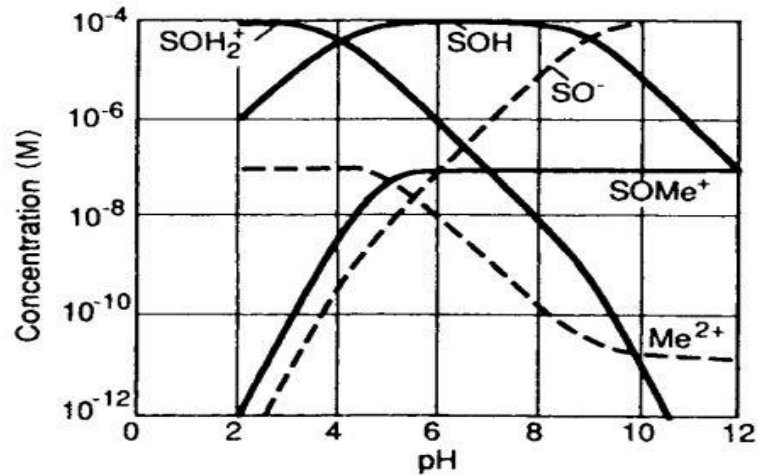


Figure 2: The existence form of the surface site over pH 0-12 (Stumm, 1995).

When ions are close to an oppositely charged surface, they are attracted to the surface due to the columbic forces. Meanwhile, the kinetic energy of the ions leads them to drift in all directions and essentially move away from the surface. Therefore, the ions form a diffusion layer near the surface. Based on Boltzmann's equation, the concentration of ions reaches maximum when they are adjacent to the surface while decreases as they move away from the surface (Vilks & Yang, 2018).

(Stern, 1924) proposed the existence of a monolayer that is restricted by the size of the adsorbed ion and surface area between the interface, and these ions are with specific adsorption potential. While the other region is the diffuse layer, only restricted by charge. Figure 3 below presents the stern layer.

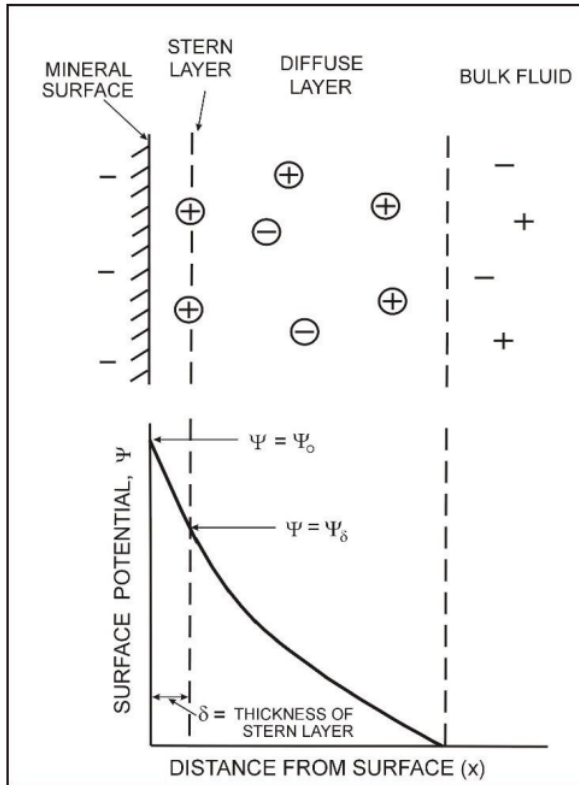


Figure 3: The schematic of the Stern layer (Stern, 1924).

Generally, the non-specific coulombic sorption is a reversible process as there is no chemical bond formed during sorption. It can be considered as an ionic exchange reaction. For example, a cation can be sorbed by replacing another cation present in the diffusion layer and stern layer of the solid surface. Also, these interactions consider the ions as point charges, thus as the salt concentration increases, the cations from the salt could potentially replace the sorbed cation. Therefore, the ionic exchange reactions might not occur in solutions with high concentration of salt, namely brine solution, but mostly occur in relatively low IS solutions. In this work, the ionic exchange reactions are considered in the sorption modeling, particularly for low ionic strength conditions.

2.1.2 Specific sorption

As mentioned in 2.1.1, the protolysis constant of a surface site is intrinsic to the mineral, and the surface charge can be positive at low pH or negative at high pH region. If the sorption is purely controlled by charge, the sorption should only occur for all the metal cations within a narrow pH range at which the surface is being dominated by negative charges. However, as shown in Figure 4, the sorption of various metals onto hydrous ferric oxide exhibits a different phenomenon, in which the sorption peak of each metal occurs at different pH values. Thus, there must be other mechanisms accounting for the sorption.

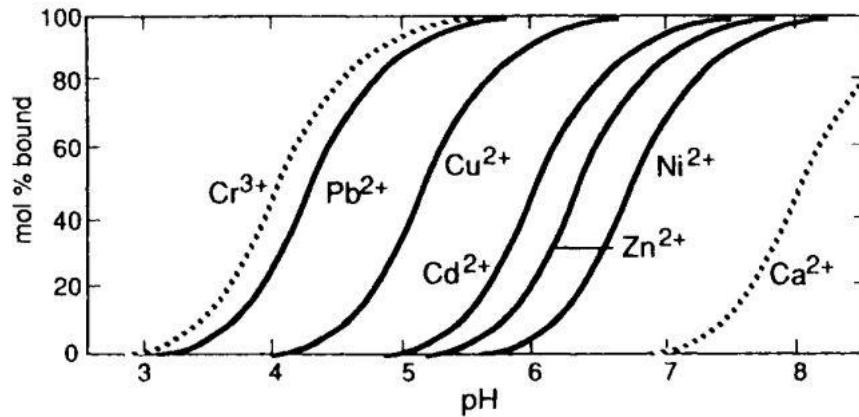


Figure 4: The pH dependence of the binding of metal ions (Stumm, 1995).

Surface complexation is commonly used to elucidate the specific chemical sorption. It basically involves a metal coordination with the surface ligands, forming a chemical bond. The edge of the broken bond contains oxygen atoms that could bond with H^+ from the surrounding water. Then, the cations can sorb and replace the H^+ from the surface, dependent on the pH and composition of the solution. As shown in Figure 5, the

reaction can form either an inner-sphere complex or an outer-sphere complex. In the inner-sphere complex context, there is a direct chemical bond being formed between the ion and the surface, whereas in the outer-sphere complex, an ion is attracted to an oppositely charged surface at a critical distance – which can be viewed similarly as the ions held by coulombic forces within the stern layer. Usually, there are one or more water molecules surrounding the cations that separates it from the surface. Therefore, the inner-sphere complex is stronger and usually considered as strong site complex while the outer-sphere is referred to weak site complex. The surface complexation reactions have a pH dependence.

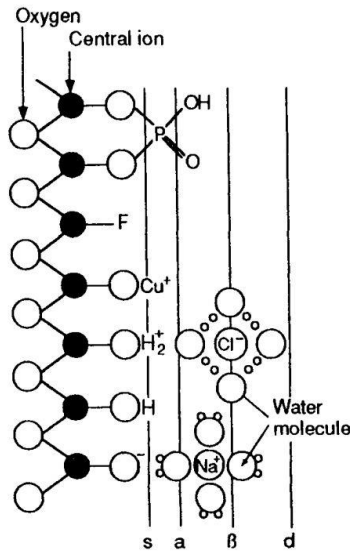


Figure 5: Schematic of Surface complex formation. “s” stands for the surface hydroxyl group, “a” represents inner-sphere complexes, “β” is outer-sphere complexes, and “d” is diffusion ion swarm (Stumm, 1995).

2.2 Experiment setup

In this work, the experimental method is batch experiment. It is one of the most common approaches to measure the adsorption equilibrium of the solids in solutions (Brandani, 2021). The schematic of the setup is shown in Figure 6. Basically, a fixed volume of solution with an initial concentration is placed in a vessel – a 15 ml test tube in this work. A certain mass of sample (MX-80 bentonite or granite in this work) is added into the tube. In this work, the solid directly contacts with the solution.

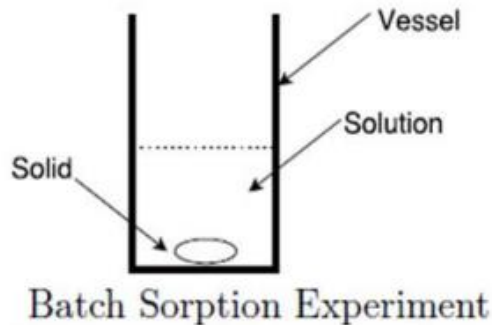


Figure 6: The schematic of batch sorption experiment method (Riddoch, 2016).

The sorption effect is usually quantified by a sorption coefficient value, “ K_d ”. As it is difficult to directly measure the amount of sorbent on the solid, K_d utilizes the concentration of the element of interest and defines a ratio between the initial concentration and the concentration at equilibrium to quantitatively calculate the sorption results. The K_d value is calculated by equation (2.4),

$$K_d = \frac{c_i - c_e}{c_e} \times \frac{L}{S} \quad (2.4)$$

Where c_i stands for the initial concentration of Eu in the solution (mol/L), c_e represents the concentration of Eu at the equilibrium (mol/L), L is the volume of the solution (m^3), and S is the mass of the solid (kg). The unit of K_d is m^3/kg .

2.3 Sorption modelling

A sorption modeling is applied to help explore the sorption mechanism and predict the sorption effects under different conditions. Both the non-specific sorption and chemical specific sorption mentioned in section 2.1 are considered in this work. The modeling is then used to fit with the experimental data. If the modeling matches with the experimental data, it is a positive indication that the sorption reactions used in the model might be the mechanisms in the experiment.

The software used in this work is PHREEQC version 3.7.3. PHREEQC version 3 is a computer program that can conduct various aqueous geochemical calculations and simulate chemical reactions and processes in water, in laboratory experiments, or in industrial processes (Parkhurst & Appelo, 2013). There are various databases that can be used in PHREEQC program such as JAEA database.

In the PHREEQC program, the sorption reactions can be modeled as surface complexation reaction or ion exchange reaction. Before conducting the actual modeling, it is always important to understand the speciation of the solution as the speciation calculation provides all the activities for the species of the interested elements in the solution as well as their concentrations. The essential data needed for the speciation calculation include temperature, pH value, and concentrations of the elements. In the

PHREEQC calculation, the activity, activity coefficients, molality, and moles in the solution would be calculated for each aqueous species.

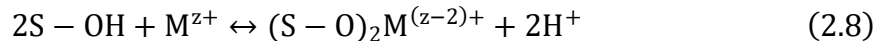
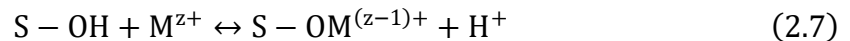
2.3.1 Surface complexation reactions modeling

As mentioned in section 2.1, the specific chemical sorption can be characterized as a surface complexation reaction. In the modeling, various surface complex formation equilibria taken from (Stumm, 1995) can be applied, as shown in equations (2.5) – (2.13).

Acid-Base Equilibria



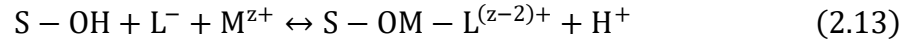
Metal Binding (M^{z+} = metal)



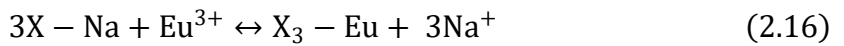
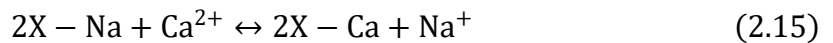
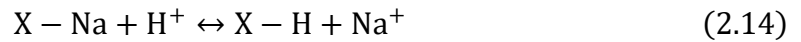
Ligand Exchange (L^- = ligand)



Ternary Surface Complex Formation

**2.3.2 Ionic exchange reactions**

Similarly, the coulombic sorption can be viewed as an ion exchange reaction. As mentioned in section 2.1, the ionic exchange is a completely reversible reaction as the ions can be replaced by other ions. This effect is also considered while modeling the sorption of Eu onto both granite and MX-80 bentonite in the Ca-Na-Cl solutions. The equilibria considered are as follows:



3 Experimental Methods

3.1 Materials & Equipment

The Granite is obtained from Manitoba, Canada. The MX-80 bentonite is purchased from American Colloid Company. The granite was crushed and sieved by a 150-300 μm sieve, while the MX-80 bentonite was used as received.

NaCl powder and $\text{CaCl}_2 \cdot 2\text{H}_2\text{O}$ are used to make the Ca-Na-Cl solution at different ionic strength. HCl and NaOH were purchased from Fisher company, serving as buffer solutions to adjust pH conditions. The Eu stock solution, 1000 $\mu\text{g}/\text{ml}$ in 5% HNO_3 , is purchased from Agilent Technologies. The balance is obtained from Sartorius, with an accuracy of 0.0005g. The pipettes used in this experiment were purchased from Fisher company. To achieve the reducing conditions, all experiments were performed in a N_2 -filled glove box obtained from Inert company. A centrifuge obtained from Beckman Coulter was used to centrifuge the samples and separate the liquid from solid debris. The concentration of samples was measured by a Triple Quad 8800 inductively coupled plasma mass spectrometry (ICPMS) from Agilent Technologies.

3.2 Preparation of solutions

The Ca-Na-Cl solutions were prepared for the sorption experiments. The NaCl and $\text{CaCl}_2 \cdot 2\text{H}_2\text{O}$ powders were mixed with deionized water, with a Na/Ca mass ratio of 1.55M. The composition of the solutions for each ionic strength is listed in Table 1.

Table 1: The salt masses of Ca-Na-Cl solutions for each ionic strength

Ionic Strength of the solution (M)	NaCl (g/L)	CaCl ₂ *2H ₂ O (g/L)
0.05	0.9954	1.6155
0.1	1.9908	3.2309
0.24	4.7779	7.7543
0.5	9.9540	16.1547
1	19.9081	32.3095

Then, the Eu will be added to the Ca-Na-Cl solutions with an initial concentration of $1 \times 10^{-6} M$.

3.3 Detection limit of Eu (III)

The detection limit of ICPMS on Eu concentrations needs to be measured experimentally. This measurement can help determine the lowest concentration of Eu that can be detected by the ICPMS, and further help determine the suitable Eu concentration used in the experiment.

The method is to measure solutions with various Eu concentrations by ICPMS. Basically, the ICPMS measures the concentration of each sample and provides a count per second (CPS). The DI water will also be used as a background to help examine the detection limit of Eu. For instance, if the CPS of the DI water is about 13 (normally at 10th magnitude) while one solution with Eu has a CPS of 130, it could be considered as

effective measurement of Eu concentration. However, if the CPS of Eu in solution is around 30 or 50, it would be difficult to distinguish between DI water and the element, thus this specific concentration would be considered as the limit bound. Solutions with Eu concentrations of 10^{-7} , 10^{-8} , 10^{-9} , 10^{-10} , 10^{-11} , 10^{-12} , and 10^{-13} were prepared in DI water. For this work, the detection limit for Eu was measured by (Yang et al., 2022) which found that the lowest Eu concentration that can be effectively measured by the ICPMS is around 10^{-11} mol/L.

3.4 Eu (III) Solubility

The solubility of Eu in Ca-Na-Cl solution needs to be determined in terms of concentration. This helps to determine the highest Eu concentration can be used in this research, thus determining the suitable Eu concentration.

The method is to measure Eu concentration in Ca-Na-Cl solutions by ICPMS and observe its stability over a 21-day period. The Ca-Na-Cl solutions with Eu ionic strength of 0.05M and 1M were prepared. The Eu concentration is set to be 10^{-4} mol/L. The supernatant solution of each sample is taken for ICPMS on day 1, 2, 6, 10, 14, and 21 to observe the variation of Eu concentrations in the solution. Combining with the solubility of Eu in Na-Ca-Cl solution by (Yang et al., 2022), the concentration of Eu for this experiment can be determined.

3.5 Eu (III) Kinetics

The kinetics experiment needs to be conducted to help determine the equilibrium period for Eu sorption on each rock. Batch experiment method is applied in the

experiment. The solid/liquid ratio is set to be 20mg/10ml. The lowest and highest tested ionic strengths are 0.05M and 1M.

The kinetics of Eu onto granite and MX-80 bentonite was determined to be 14 days based on the results from (Yang et al., 2022). Basically, 20 mg of the solids – MX-80 bentonite and granite – are added to a 15 ml test tube. The solids will be preconditioned by Ca-Na-Cl solutions for 5-7 days, after which 10 ml Ca-Na-Cl solution with Eu are added to the test tube. The supernatant solution for each ionic strength was taken on day 1, 2, 4, 6, 10, 15, 20, 25, 30, and 40, and centrifuged at 18000 rpm for 30 minutes. Then the samples are diluted by a factor of 20 times with DI water.

3.6 pH and ionic strength dependence of Eu (III) sorption

The sorption experiment was conducted over pH of 4 to 9 and various ionic strength of Ca-Na-Cl solutions, including 0.05m, 0.1m, 0.24m, 0.5m, and 1m. The initial concentration of Eu was $1 \times 10^{-6} M$. The solid and liquid ratio was set to be 10mg/10ml. The solid and solutions were added to a polypropylene test tube for each condition. Based on the kinetics, the equilibrium period was set to be 14 days for both the sorption onto granite and MX-80 bentonite. All the experiments were performed in a N₂-filled glove box to ensure the reducing condition.

Initially, the solid was preconditioned using pure Ca-Na-Cl solutions, with a solid/liquid ratio of 5mg/10ml. After 5-7 days of standing, the samples were centrifuged at 5860 rpm for 6 minutes, followed which the liquid is taken out by a pipette. Then, the

Ca-Na-Cl solution with Eu will be added to the solid and stand for 14 days to reach equilibrium. During the period of reaction, the pH of the solution is regularly adjusted to ensure the desired condition and the Eh was measured to confirm the oxidation state of the Eu. After 14-day of standing, the supernatant solution of each sample was transferred to a centrifuge tube. Samples were centrifuged at 18,000 rpm for 30 minutes to separate the solid and liquid. The supernatant solution was diluted 20 times for the 1 m solution, and 10 times for other solutions. A 13mm syringe filter was then applied to ensure sufficient separation of the solid and liquid. Finally, the prepared samples were transferred to the inductively coupled plasma mass spectrometry (ICPMS) for Eu concentration measurement.

As mentioned in the theory section, the ionic exchange reactions are expected to occur at low pH region and relatively low ionic strength conditions. The effect of ionic strength is observed at around the same pH region. Namely, fix a pH point and observe the results at different ionic strength.

4 Sorption modeling

In this study, PHREEQC Version 3 software with Notepad++ was used to model the sorption of Eu (III) onto granite and MX-80 bentonite.

4.1 Thermodynamic data

Table 2 below demonstrates the initial concentration of the Ca-Na-Cl solutions with Eu. In this work, the Ca-Na-Cl solution is referred to as the CR-10 groundwater type and has a Na/Ca ratio of 1.55. Various ionic strengths from 0.05 m to 1 m are included. The initial redox condition is set to be 3.5 and pH is 6.0, based on the CR-10 groundwater type.

Table 2: The ion concentration of Ca-Na-Cl solutions for each concentration.

Master Species	Initial concentrations (m)				
	<i>I = 0.05 m</i>	<i>I = 0.1 m</i>	<i>I = 0.24 m</i>	<i>I = 0.5 m</i>	<i>I = 1 m</i>
Na ⁺	0.017033	0.0340659	0.0817582	0.1703297	0.3406593
Ca ²⁺	0.010989	0.021978	0.0527473	0.1098901	0.2197802
Cl ⁻	0.039011	0.078022	0.1872527	0.3901099	0.7802198
Eu ³⁺	10 ⁻⁶	10 ⁻⁶	10 ⁻⁶	10 ⁻⁶	10 ⁻⁶

These species will be included as the main aqueous species in the model. Aqueous species that may likely to form are referenced from the JAEA database (Kitamura et al.,

2014), (Spahiu & Bruno, 1995), and (Tertre et al., 2006). All are presented in Table 3, together with associated formation reactions.

Table 3: Formation reactions and associated constants of the relevant species from JAEA database (Kitamura et al., 2014) and (Spahiu & Bruno, 1995).

Formation reaction	Log K	Error
$\text{H}_2\text{O} - \text{H}^+ \leftrightarrow \text{OH}^-$	-14.001	0.015
$2\text{H}_2\text{O} - 4\text{H}^+ - 4\text{e}^- \leftrightarrow \text{O}_2$	-86.080	-
$\text{Ca}^{2+} + \text{H}_2\text{O} - \text{H}^+ \leftrightarrow \text{CaOH}^+$	-12.850	0.500
$\text{Cl}^- + \text{H}_2\text{O} - 2\text{H}^+ - 2\text{e}^- \leftrightarrow \text{ClO}^-$	-57.933	0.170
$\text{Cl}^- + 2\text{H}_2\text{O} - 4\text{H}^+ - 4\text{e}^- \leftrightarrow \text{ClO}_2^-$	-107.874	0.709
$\text{Cl}^- + 3\text{H}_2\text{O} - 6\text{H}^+ - 6\text{e}^- \leftrightarrow \text{ClO}_3^-$	-146.238	0.236
$\text{Cl}^- + 4\text{H}_2\text{O} - 8\text{H}^+ - 8\text{e}^- \leftrightarrow \text{ClO}_4^-$	-187.785	0.108
$\text{Cl}^- + \text{H}_2\text{O} - \text{H}^+ - 2\text{e}^- \leftrightarrow \text{HClO}$	-50.513	0.109
$\text{Cl}^- + 2\text{H}_2\text{O} - 3\text{H}^+ - 4\text{e}^- \leftrightarrow \text{HClO}_2$	-105.913	0.708
$\text{Eu}^{3+} + \text{OH}^- \leftrightarrow \text{Eu}(\text{OH})^{2+}$	6.2	-
$\text{Eu}^{3+} + 2\text{OH}^- \leftrightarrow \text{Eu}(\text{OH})_2^+$	11.6	-
$\text{Eu}^{3+} + 3\text{OH}^- \leftrightarrow \text{Eu}(\text{OH})_3$	16.8	-
$\text{Eu}^{3+} + \text{Cl}^- \leftrightarrow \text{EuCl}^{2+}$	0.34	-
$\text{Eu}^{3+} + 2\text{Cl}^- \leftrightarrow \text{Eu}(\text{Cl})_2^+$	-0.05	-

The activity coefficient of the aqueous species can be calculated using the Specific Ion Theory (SIT). The JAEA thermodynamic database includes SIT parameters for many aqueous species. However, JAEA TDB does not contain the relevant data of Eu and given that Am shares similar sorption properties with Eu, the data of Am is applied in the model to simulate the reactions. Table 4 below lists the SIT parameters for relevant species.

Table 4: SIT parameters for the species in this modeling (Kitamura et al., 2014).

Species 1	Species 2	Epsilon	Error
H ⁺	Cl ⁻	0.12	0.01
OH ⁻	Na ⁺	0.04	0.01
Cl ⁻	Na ⁺	0.03	0.01
Ca ²⁺	Cl ⁻	0.14	0.01
Eu ³⁺	Cl ⁻	0.23	0.02
Eu(OH) ²⁺	Cl ⁻	-0.04	0.07
Eu(OH) ₂ ⁺	Cl ⁻	-0.27	0.2

4.2 Surface definition

The reaction surface is modeled in the SURFACE block to set the sorption sites and relevant properties, including specific surface area (m²/g), surface sites (mol/g), and the mass of the solid(g). For the surface site, both the strong and weak sites are considered in the modeling.

In this research, the granite surface was modeled using component activity (CA) method. Namely, each main component of the granite is considered and modeled. The composition of granite mainly includes feldspar (61.8%), quartz (29.4%), and biotite (5.4%). The parameters including specific surface area (SSA) were taken from (Iida et al., 2016), Table 5 presents the components defined in the modeling. The solution used in the model is 1 L and the mass of the solid is 1 g.

Table 5: Defined surface site in the modeling for granite. “_sOH” stands for strong site while “w_OH” stands for weak site. “Surf_xNa” represents the ionic exchange site (Iida et al., 2016).

Site_Name	Site (mol/g)	Specific surface area (m ² /g)	Mass (g)
Feldspar_sOH	6.725×10^{-6}	1	0.560
Biotite_sOH	2.7205×10^{-5}	4.3	0.03
Quartz-sOH	6.5908×10^{-6}	0.7	0.34
Biotite_wOH	1.39×10^{-5}	4.3	1
Surf_xNa	9.3×10^{-5}	1.056	0.93

As for the MX-80 bentonite, since the main component is determined to be montmorillonite, the model considers the surface as a whole and simulates the sorption of

Eu onto the montmorillonite. The site was referenced from (Grambow et al., 2006). Table 6 demonstrates the defined surface for MX-80 bentonite in the modeling.

Table 6: Defined surface site in the modeling for MX80-bentonite. “_sOH” stands for strong site while “w_OH” stands for weak site. “ww_OH” stands for the second weak site considered in the model. “Surf_xNa” represents the ionic exchange site (Grambow et al., 2006).

Site_Name	Site (mol/g)
Surf_sOH	2.5×10^{-6}
Surf_wOH	3.2×10^{-5}
Surf_wwOH	3.2×10^{-5}
Surf_xNa	6.96×10^{-4}

4.3 Surface complexation reaction & Ionic exchange reactions

As mentioned in section 2.3, this work considers the surface complexation reaction in the modeling. First, protonation and deprotonation will take place on the surface sites which will then be positively or negatively charged, respectively. For granite, the surface complexation constants of these reactions are obtained from (Iida et al., 2016). For MX-80 bentonite, these constants are from (Bradbury & Baeyens, 2005). Table 7 and 8 present the protonation and deprotonation reactions of the granite site and MX-80 bentonite site considered in this model, respectively.

Table 7: The protonation and deprotonation reactions for the components of granite (Iida et al., 2016).

Surface protolysis reactions	<i>LogK</i>
Feldspar_sOH \leftrightarrow Feldspar_sO ⁻ + H ⁺	-8.46
Feldspar_sOH + H ⁺ \leftrightarrow Feldspar_sOH ₂ ⁺	4.13
Biotite_sOH + H ⁺ \leftrightarrow Biotite_sOH ₂ ⁺	6.06
Biotite_sOH \leftrightarrow Biotite_sO ⁻ + H ⁺	-9.00
Quartz_sOH + H ⁺ \leftrightarrow Quartz_sOH ₂ ⁺	-1.10
Quartz_sOH \leftrightarrow Quartz_sO ⁻ + H ⁺	-7.20
Biotite_wOH + H ⁺ \leftrightarrow Biotite_wOH ₂ ⁺	4.60
Biotite_wOH \leftrightarrow Biotite_wO ⁻ + H ⁺	-8.40

Table 8: The protonation and deprotonation reactions with associated constants for the montmorillonite (Bradbury & Baeyens, 2005).

Surface protolysis reactions	<i>LogK^S</i>	<i>LogK^{W1}</i>	<i>LogK^{W2}</i>
S-OH + H ⁺ \leftrightarrow S-OH ₂ ⁺	4.5	4.5	6.0
S-OH \leftrightarrow S-O ⁻ + H ⁺	-7.9	-7.9	-10.5

5 Results and Discussion

This chapter presents the experimental results and modeling results of this work. The effects of pH and ionic strength are discussed in the section below. The modeling helps verify the experimental data and illustrate possible mechanism occurred during the sorption event. Additionally, the solubility of the Eu in Ca-Na-Cl solutions is also showed, which helped understand the stable concentration of Eu in Ca-Na-Cl solutions and determine the suitable concentration for the experiment.

5.1 Solubility

Figure 7 shows the solubility of Eu in both 0.05 m and 1 m Ca-Na-Cl solutions. The initial concentration of Eu was set to be 10^{-4} mol/L. In general, the concentration of Eu in both solution types experienced a sharp decline over the first 2 days and then tended to be plateau starting from day 6. In 1 m Ca-Na-Cl solution, the Eu concentration reaches about 10^{-5} mol/L on day 6 and remains constant. While for 0.05 m solution, the Eu concentration is about $0.8 \cdot 10^{-5}$ mol/L on day 6 and tends to stay around this value. The result indicates that 10^{-4} mol/L is above the solubility limit of Eu in Ca-Na-Cl solution, while $0.8 \cdot 10^{-5}$ mol/L could be an upper limit when selecting the Eu concentration for the experiment. Combining with detection limit of Eu by ICPMS and the solubility of Eu in Na-Ca-Cl solution done by previous work (Yang et al., 2022), the Eu concentration was set to be 10^{-6} mol/L in this work.

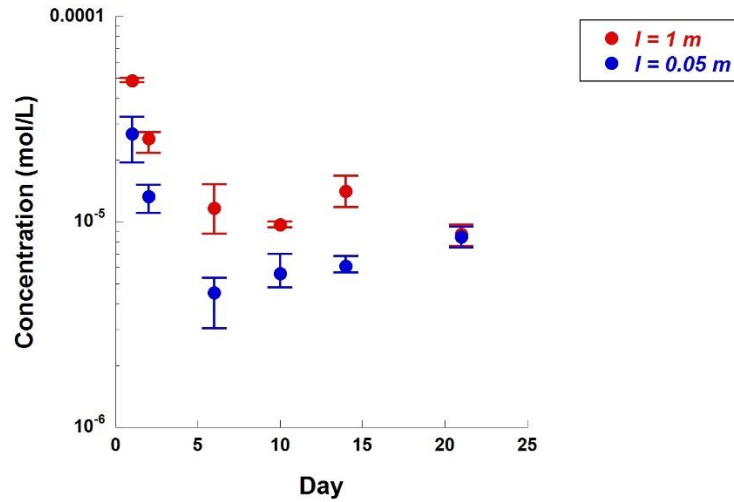


Figure 7: Solubility of Eu in 0.05 m and 1 m Ca-Na-Cl solutions over a 21-day period.

5.2 pH dependence and ionic strength dependence of Eu (III) sorption

Figures 8 and 9 demonstrate the experimental results of Eu sorption onto both granite and MX-80 bentonite, as a function of pH_m , respectively. The pH_m ranges from 4-9 and the ionic strength includes 0.05 m, 0.1 m, 0.24 m, 0.5 m, and 1 m.

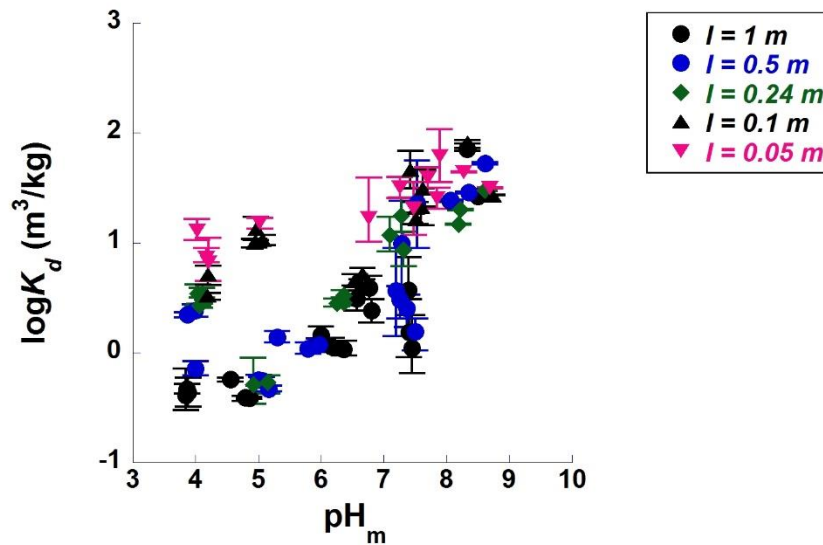


Figure 8: Experimental results for sorption of Eu onto granite.

For granite, the sorption results showed a clear pH dependence. It firstly tends to be constant at the lower pH_m region ($pH_m < 6$) – acid region to near neutral region, and then dramatically increase until around $pH\ 8 - 9$. At $I = 0.5\text{ m}$ and 1 m , the K_d value remains almost constant from $pH\ 4$ to $pH\ 5$, followed by a sharp increase to $pH\ 8$. While for $I = 0.05\text{ m}$, 0.1 m , and 0.24 m , the K_d value seems to stay constant over a longer pH_m range as the K_d value starts to increase at around $pH\ 6$.

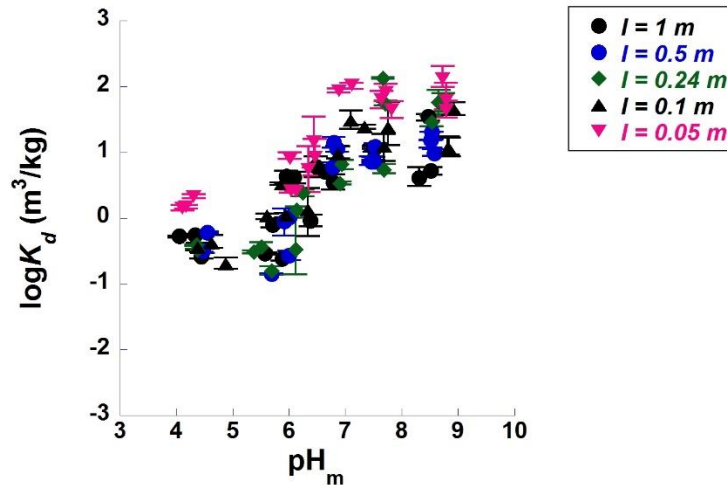


Figure 9: Experimental results for sorption of Eu onto MX-80 bentonite.

For MX-80 bentonite, a similar trend is observed that the K_d value also tends to remain constant at lower pH region and experienced an increase to around pH 9. It is also clear that the sorption is strongly dependent on pH as the K_d value increases with pH increasing.

As each sample was measured three times by the ICPMS, there were three data points collected for each sample. The error bar was then calculated by the difference between the average value and maximum/minimum value of the three data points.

The effects of the ionic strength on the sorption can also be observed from the results. For the sorption of Eu onto granite, as shown in Figure 8, the K_d value is larger at smaller ionic strength in the acidic region, whereas at the higher pH region, the K_d value

tends to be independent of the ionic strength as it is at similar level for all I . To have a clearer observation, Figure 10 below presents the K_d results at around pH 4 and pH 5 for the Eu sorption onto granite. Figure 11 shows K_d at around pH 8-9, both as a function of ionic strength. At around pH 4 and 5, K_d experienced a dramatic decrease as the ionic strength increases. While as the pH condition rises to around 8 and 9, the ionic strength does not exhibit significant effects on the sorption, and the K_d value for each ionic strength condition is at the same level.

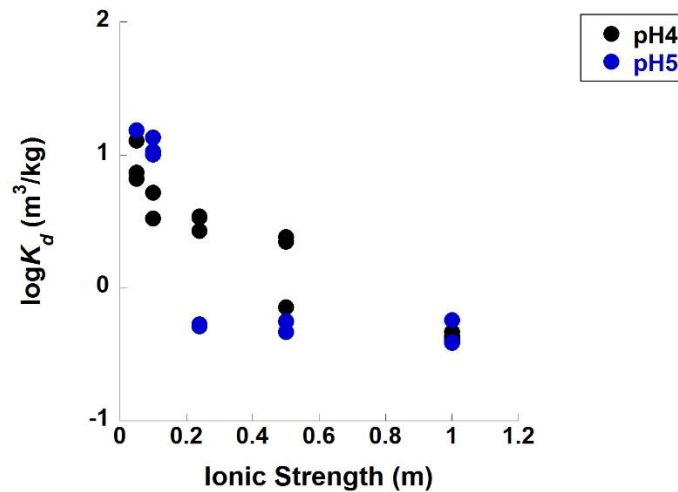


Figure 10: The sorption coefficient value K_d for Eu sorption onto granite as a function of ionic strength at around pH4 and pH5.

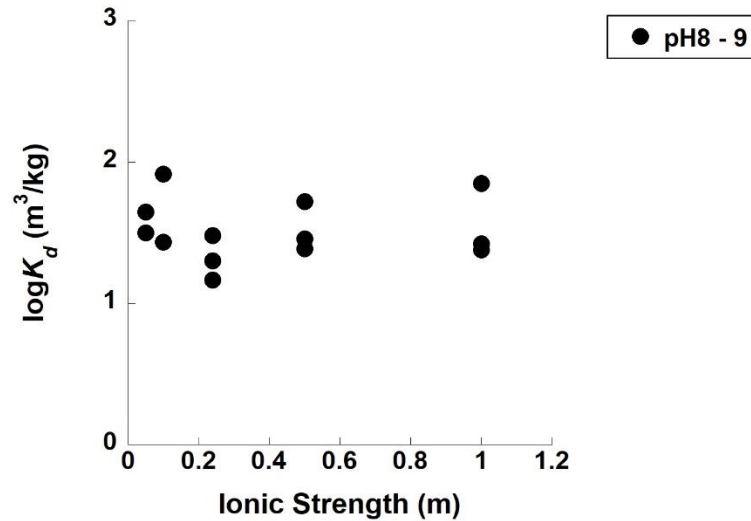


Figure 11: The sorption coefficient value K_d for Eu sorption onto granite as a function of ionic strength at around pH8-9.

In terms of Eu sorption onto MX-80 bentonite, the ionic strength exhibits little effect on the sorption, mostly around lower pH region. From Figure 9, it is clear that at pH 4-5, the K_d value tends to be larger at lower ionic strength condition. Figure 12 below presents the K_d value as a function of ionic strength at around pH 6, 7, and 8. The result indicates that the ionic strength exhibits little effect at pH 6 while almost no effect at higher pH conditions (pH > 6), as the K_d values for each condition are at the same order of magnitude despite of ionic strength.

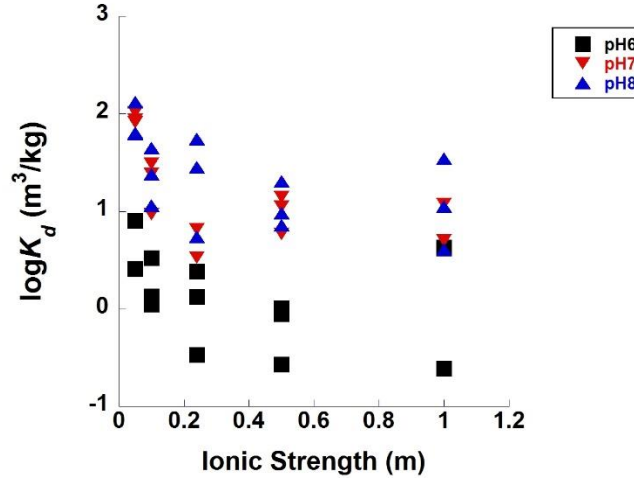


Figure 12: The sorption coefficient value K_d for Eu sorption onto MX-80 bentonite as a function of ionic strength at around pH 6,7,8.

From chapter 2, the strong pH dependence of Eu sorption onto both granite and MX-80 bentonite indicates that the surface complexation reactions occur and dominate. Based on the theory, the metal at the edge of the surface can coordinate with the water molecules to form the surface $S - OH$, which then can go through protonation and deprotonation, as shown in equations (5.1) and (5.2). Figure 2 in chapter 2 also demonstrates a distribution of the surface species under different pH. At low pH region, the dominant species is $S - OH_2^+$ since hydrogen ions are dominant in solution and the reaction produces more products. Therefore, only few coordination reactions can occur since metal ions mainly coordinate with $S - OH$ which is little at this pH region. And the sorption could go through non-specific sorption which involves ionic exchange reactions and depends on the ionic strength. Since the sorption result in this work shows

dependence on ionic strength at low pH, the sorption might be attributed to the ionic exchange reactions in the lower pH region. As pH increases, $S - OH$ starts to dominate in the solution, thus metal ions can coordinate with and sorb onto the surface. The sorption result also tends to increase with pH increasing from about pH5 or 6, thus the main contribution to the sorption at higher pH might be the surface complexation.



The experimental results were also compared with available sorption data reported by other research, referenced from JAEA database. Figure 13 presents the sorption results of this work in comparison with the available sorption data of Eu sorption onto granite. Currently, there are few available data for Eu sorption onto granite, especially those that cover similar, wide pH and ionic strength range as of this work. Also, the experimental condition for most previous research is at low ionic strength such as 0.066 M and 0.1 M solutions. Therefore, the sorption results in 0.05 m and 0.1 m Ca-Na-Cl solutions from this work were used for comparison. The main experimental differences between this work and other work are solution type and rock/mineral type. Generally, the sorption results share similar trend with the results from other work, and the K_d value is within the range of available data, which indicates that the sorption data from this work is at a reasonable range.

Figure 14 shows the comparison between this work and previous research results on the sorption of Eu onto bentonite rocks. Due to most available data are obtained at low

ionic strength such as 0.1M solution, the Eu sorption in 0.1 m Ca-Na-Cl solution of this work was used for comparison. Despite the difference in the solution type, the sorption results follow a similar trend with other data. The sorption coefficient value, K_d , is within the range of the data from previous research.

The comparison with previous research data indicates that the obtained sorption results in this work are at a reasonable range and align with the trend of other data for Eu sorption. It also shows that there is few to no available data that covers the wide range of ionic strength and pH as of this work, thus the data obtained in this work could potentially provide relevant and useful information for the sorption results in high ionic strength in Ca-Na-Cl solution.

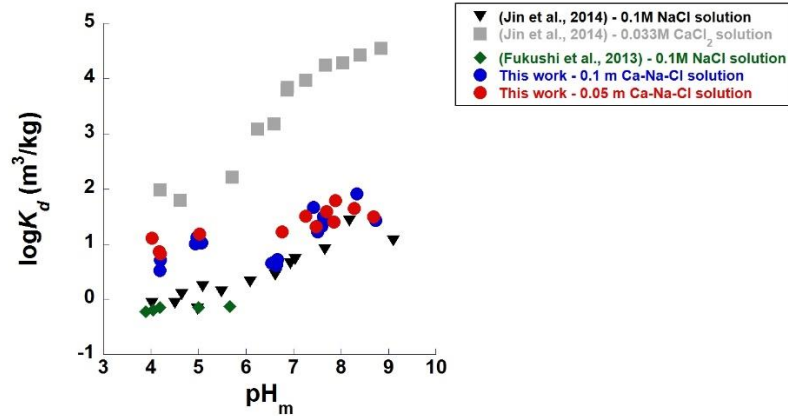


Figure 13: Comparison of sorption results onto granite with previous work. The solution type of other work include 0.1M NaCl solution and 0.033M CaCl₂ solution in (Jin et al., 2014), and 0.1M NaCl solution in (Fukushi et al., 2013), “M” stands for molarity (mol/L), “m” is molality (mol/kg).

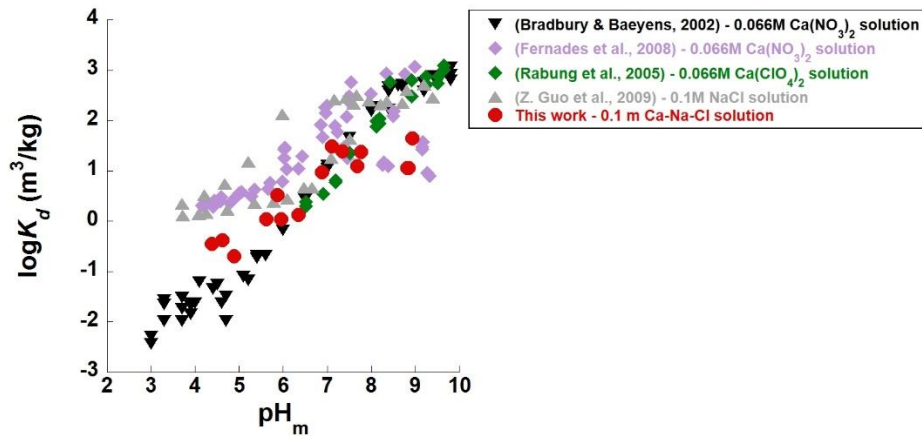
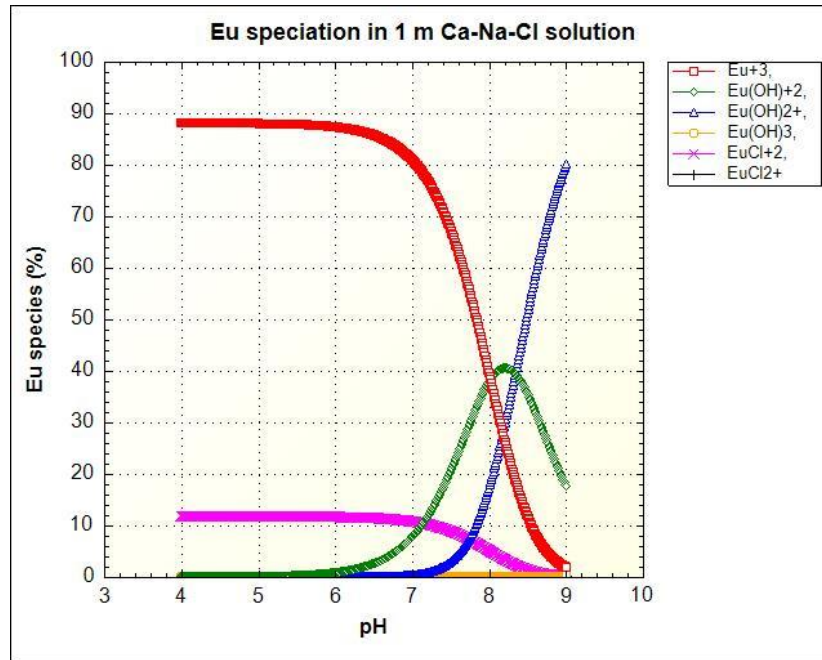


Figure 14: Comparison of sorption results onto MX-80 bentonite with other work. The solution type for other work is 0.066M Ca(NO₃)₂ in (Bradbury & Baeyens, 2002) and (Fernandes et al., 2008), 0.066M Ca(ClO₄)₂ in (Rabung et al., 2005), and 0.1M NaCl in (Z. Guo et al., 2009), “M” stands for molarity (mol/L), “m” is molality (mol/kg).

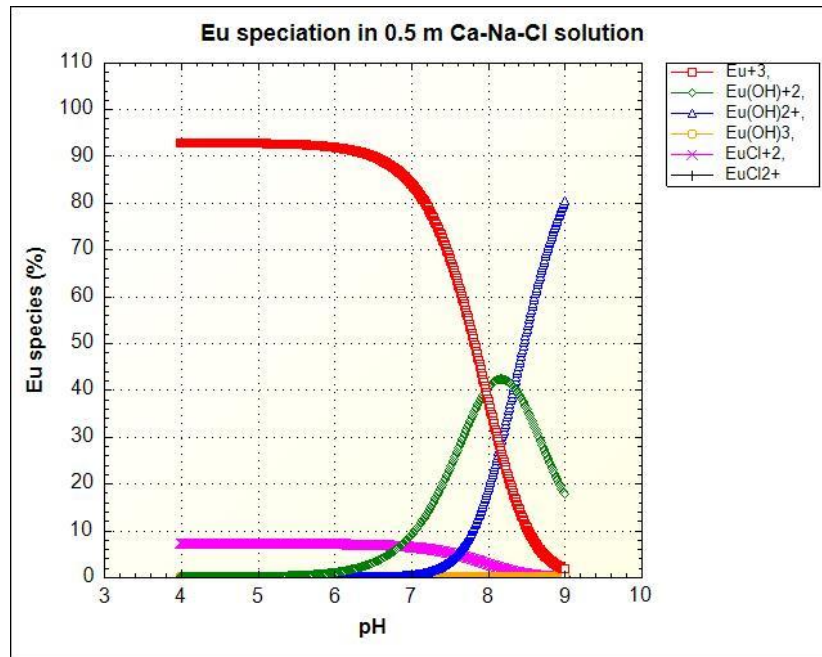
5.3 PHREEQC modeling

As mentioned in Chapter 4, a non-electrostatic sorption model was developed to help verify the experimental results and determine the possible surface complexes and reactions occurred in the experiments.

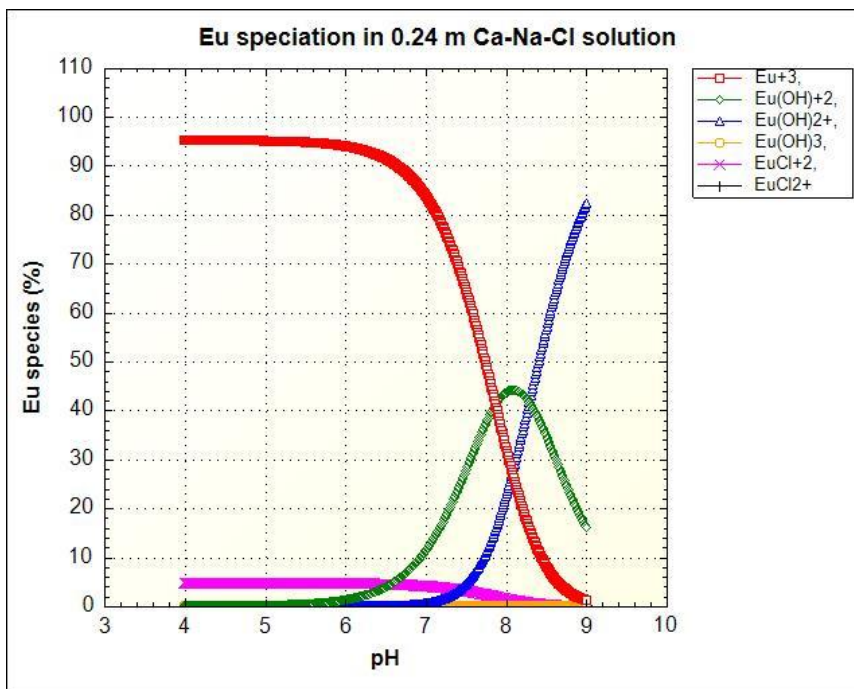
Firstly, the solution species of the Ca-Na-Cl solutions were determined based on JAEA database (Kitamura et al., 2014) and (Spahiu & Bruno, 1995). This helps to determine the possible existence of the Eu species in the Ca-Na-Cl solution with their distribution under certain pH and ionic strength conditions. Thus, the possible reactants under each condition might be identified. The Eu species in Ca-Na-Cl solutions are presented in Figure 15.



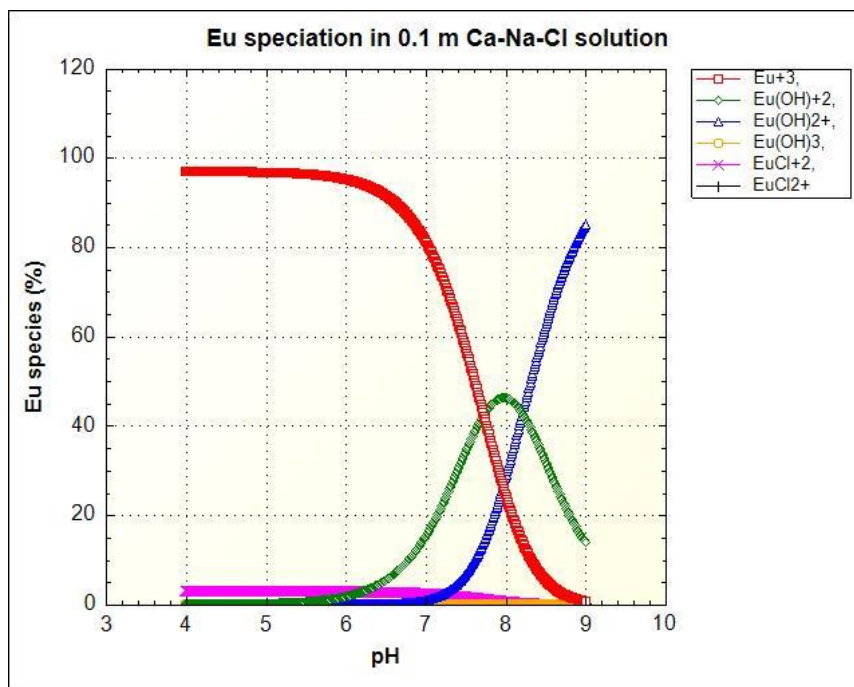
(a)



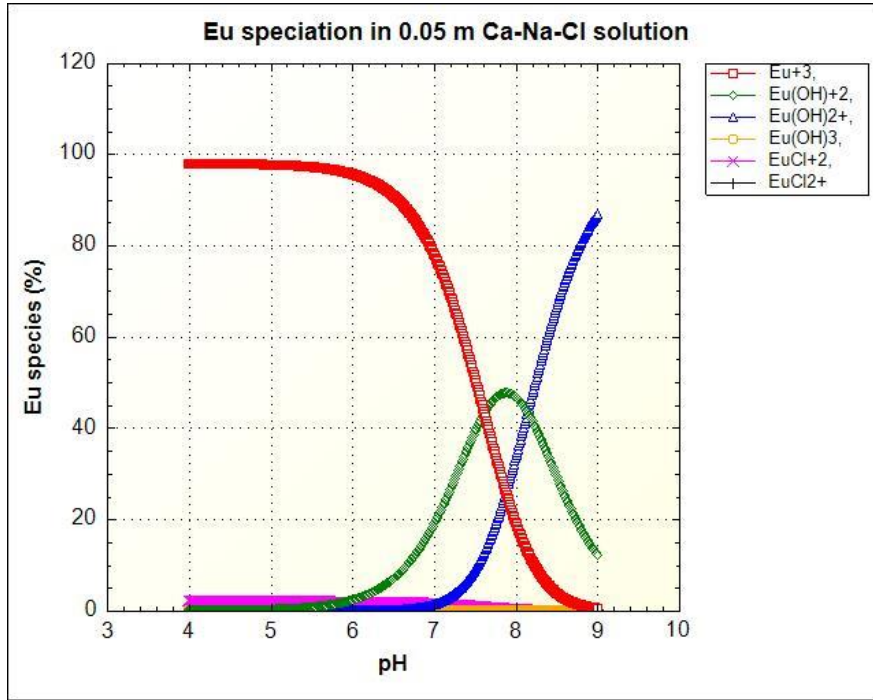
(b)



(c)



(d)



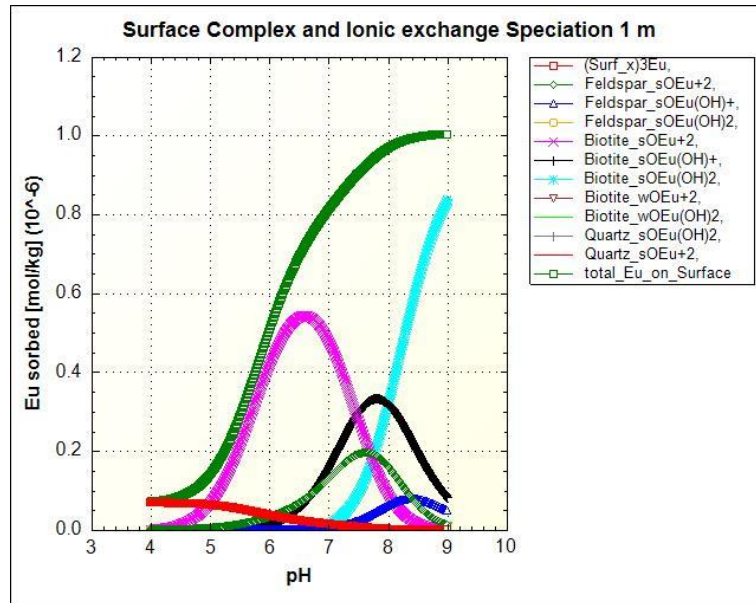
(e)

Figure 15: The solution speciation of Eu in Ca-Na-Cl solution. (a) is in 1 m solution, (b) is in 0.5 m solution, (c) is in 0.24 m solution, (d) is in 0.1 m solution, and (e) is in 0.05 m solution.

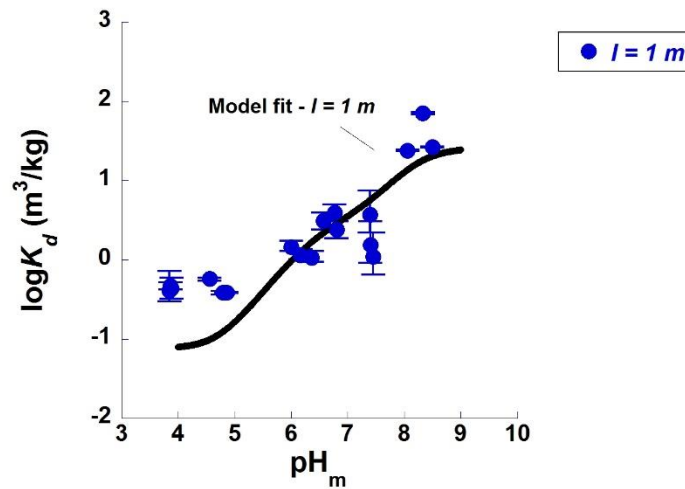
As shown in Figure 15, the main existence of Eu at acidic and neutral pH is Eu^{3+} , while Eu exists in hydroxide form as EuOH^{2+} and $\text{Eu}(\text{OH})_2^+$ at higher pH region. For higher ionic strength such as 0.5 m and 1 m, EuCl_2 is also formed at lower pH region. The Eu speciation can serve as a reference to start the modeling as it demonstrates the species of Eu with their distribution at each pH and ionic strength condition.

5.3.1 Modeling results for Eu sorption onto granite

For granite, the modeling results are shown in Figures 16-20. Each figure contains the surface complex speciation and the sorption modeling.

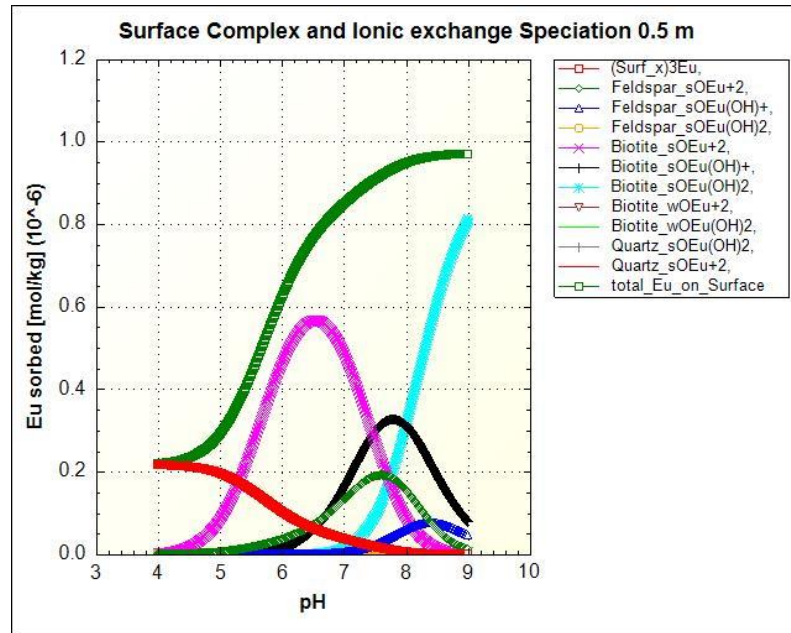


(a)

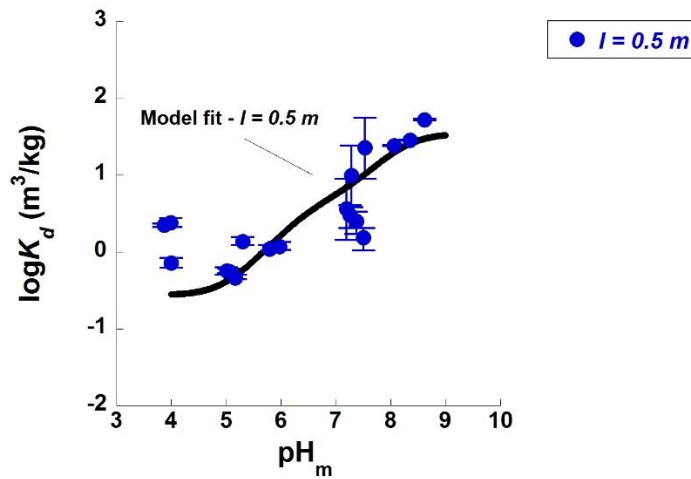


(b)

Figure 16: The sorption modeling for the sorption of Eu onto granite at 1 m Ca-Na-Cl solution. (a) is the speciation of the surface complex; (b) is the curve fitting for the experimental results.

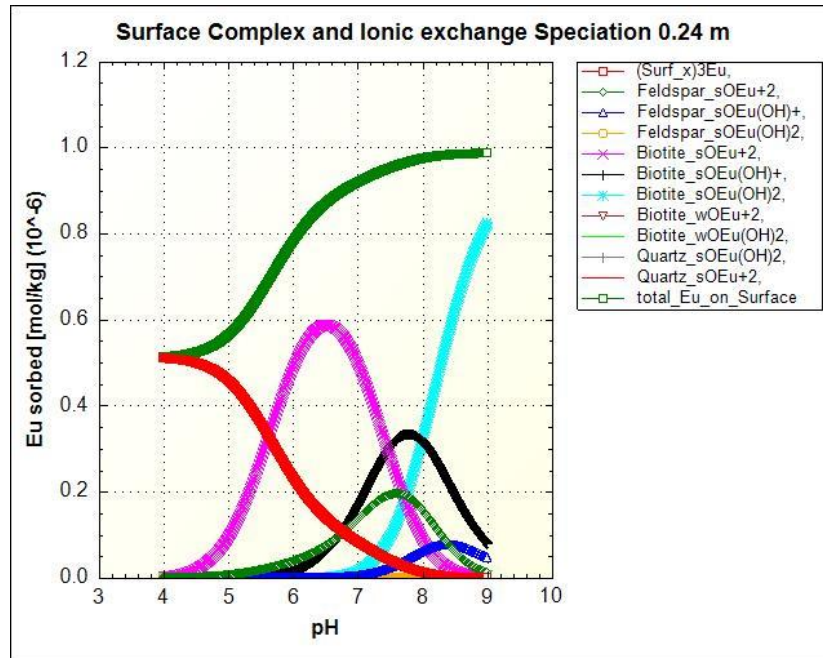


(a)

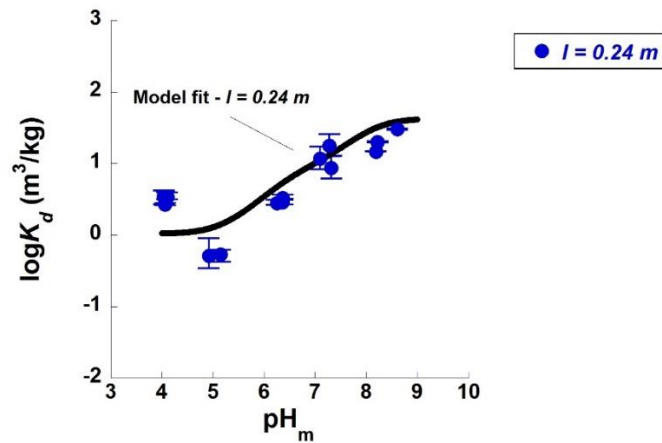


(b)

Figure 17: The sorption modeling for the sorption of Eu onto granite at 0.5 m Ca-Na-Cl solution. (a) is the speciation of the surface complex; (b) is the curve fitting for the experimental results.

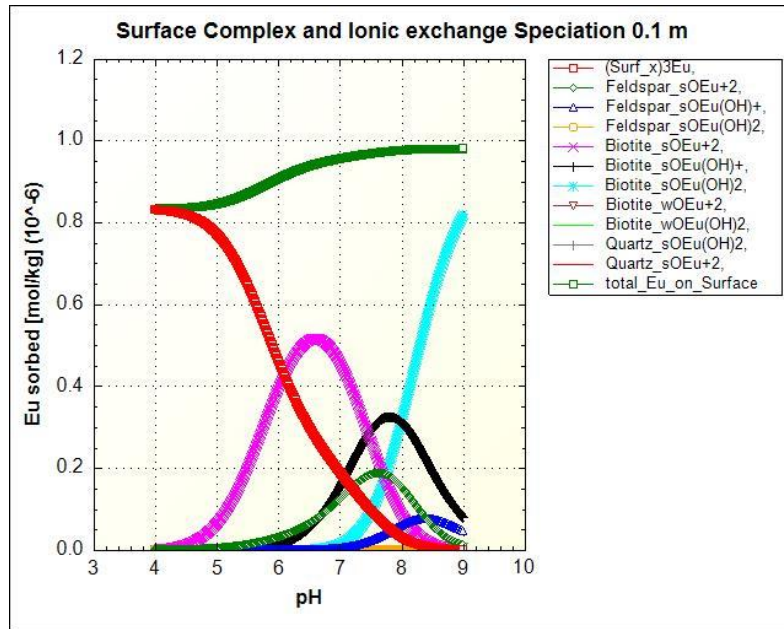


(a)

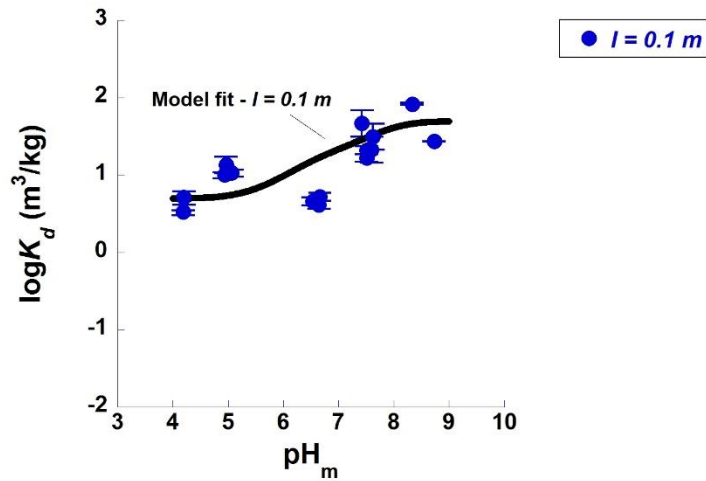


(b)

Figure 18: The sorption modeling for the sorption of Eu onto granite at 0.24 m Ca-Na-Cl solution. (a) is the speciation of the surface complex; (b) is the curve fitting for the experimental results.

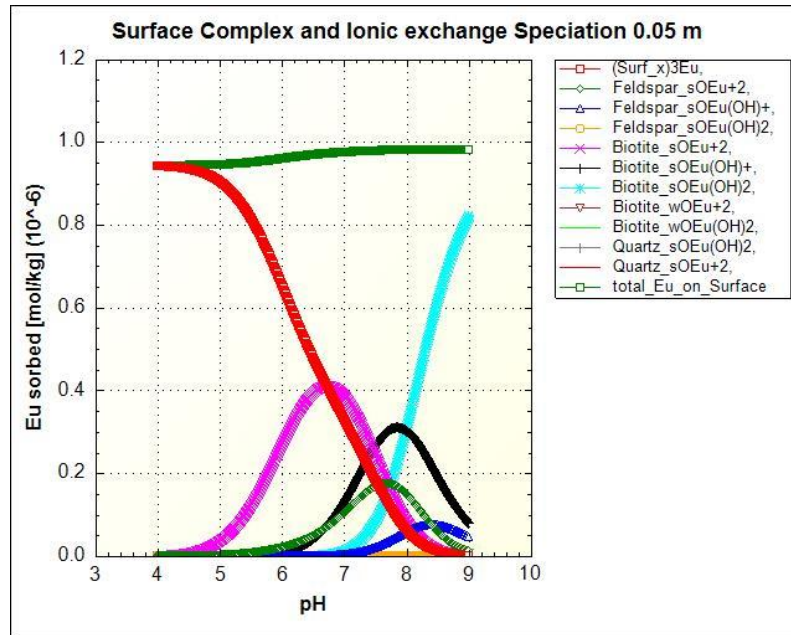


(a)

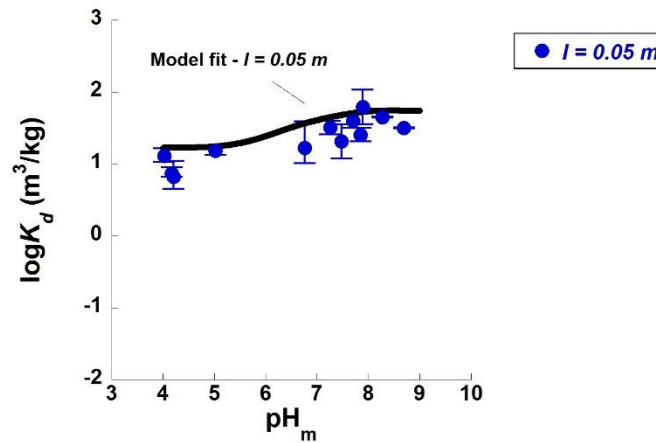


(b)

Figure 19: The sorption modeling for the sorption of Eu onto granite at 0.1 m Ca-Na-Cl solution. (a) is the speciation of the surface complex; (b) is the curve fitting for the experimental results.



(a)



(b)

Figure 20: The sorption modeling for the sorption of Eu onto granite at 0.05 m Ca-Na-Cl solution. (a) is the speciation of the surface complex; (b) is the curve fitting for the experimental results.

In this model, three main components of granite were considered, namely biotite, feldspar, and quartz. In general, the modeling curve aligns with the trend of the experimental data and fits with most data points within uncertainties. However, it was found that the modeling underestimated the experimental results at around pH 4 in 0.24 m, 0.5 m, and 1 m solutions. The model also overestimated the sorption results in 0.1 m solution at pH 6. There are several factors that might cause the discrepancies.

For the underestimation of results in 0.24 m, 0.5 m, and 1 m solutions at pH 4, it might be attributed to the EuCl_2 species that mostly occur in high ionic strength, based on the solution speciation in Figure 15. Further work is needed to examine and discuss the effect of EuCl_2 on the sorption. As for the overestimation at 0.1 m, from the surface complexes speciation figures, the ionic exchange reactions tend to occur and dominate at low ionic strength condition. It can also be seen that at pH 6, the ionic exchange reaction still contributes significantly to the sorption. Thus, the possible factor could be that the model underestimated the competitiveness of Ca^{2+} as it competes with Eu^{3+} on the ionic exchange reactions. A further work is also needed to determine the effects of Ca^{2+} in 0.1 m solution. Additionally, this modeling utilizes the component additivity (CA) method that can potentially provide the sorption information of Eu on the main components of granite. It is acknowledged that CA method usually involves many adjustable parameters. As the same chemical reactions with the reaction constants account for the experimental data over all ionic strength conditions, it is possible that many unknown adjustable parameters could lead to some discrepancies.

The surface complex speciation results suggest that the ionic exchange reactions mainly occur at acidic pH region – pH 4-6, while the surface complexation dominates at near neutral to basic pH region. At low ionic strength conditions such as 0.05 m and 0.1 m, the ionic exchange reactions dominate at pH 4-6, while the ionic exchange sorption only dominates at around pH4 for higher ionic strength such as 0.5 m and 1 m. This observation agrees with the findings of the experimental data. At higher pH region, the surface complexation accounts for the sorption since the mainly formed surface complexes include Biotite_sOEu²⁺, Biotite_sOEuOH⁺, and Biotite_sOEu(OH)₂. It can be seen that both biotite and feldspar are the contributors of the sorption. Particularly, biotite might be the main affinity of the Eu sorption onto the granite. This agrees with the findings of (Fukushi et al., 2013) and (H. Li et al., 2019), both of which found that biotite might be the main contributor of Eu sorption onto Beishan granite.

The modeling considered the sorption of Eu on feldspar, biotite, and quartz. Table 9 presents all the chemical reactions with their constants used in the model. As the modeling curve is optimized to fit with most the experiment data, the main sorption reactions are identified that can well explain the experimental results, as shown in Table 10. This can also be seen from the surface complex speciation figures as there are 6 complexes mainly formed. Also, the form of these reactions involves metal coordination, indicating that the formed complexes are mainly inner-sphere complex.

Table 9: The surface complexation and ionic exchange reactions with their constants from the optimized model.

Surface complexation and ionic exchange reactions	<i>Log_K</i>
$3\text{Surf_xNa} + \text{Eu}^{3+} \leftrightarrow (\text{Surf_x})_3\text{Eu} + 3\text{Na}^+$	7.850
$2\text{Surf_xNa} + \text{Ca}^{2+} \leftrightarrow (\text{Surf_x})_2\text{Ca} + 2\text{Na}^+$	3.180
$\text{Feldspar_sOH} + \text{Eu}^{3+} \leftrightarrow \text{Feldspar_sOEu}^{2+} + \text{H}^+$	-0.3000
$\text{Feldspar_sOH} + \text{Eu}^{3+} + \text{H}_2\text{O} \leftrightarrow \text{Feldspar_sOEu}(\text{OH})^+ + 2\text{H}^+$	-8.700
$\text{Feldspar_sOH} + \text{Eu}^{3+} + 2\text{H}_2\text{O} \leftrightarrow \text{Feldspar_sOEu}(\text{OH})_2 + 3\text{H}^+$	-19.20
$\text{Biotite_sOH} + \text{Eu}^{3+} \leftrightarrow \text{Biotite_sOEu}^{2+} + \text{H}^+$	0.3500
$\text{Biotite_sOH} + \text{Eu}^{3+} + \text{H}_2\text{O} \leftrightarrow \text{Biotite_sOEu}(\text{OH})^+ + 2\text{H}^+$	-7.120
$\text{Biotite_sOH} + \text{Eu}^{3+} + 2\text{H}_2\text{O} \leftrightarrow \text{Biotite_sOEu}(\text{OH})_2 + 3\text{H}^+$	-15.10
$\text{Biotite_wOH} + \text{Eu}^{3+} \leftrightarrow \text{Biotite_wOEu}^{2+} + \text{H}^+$	-5.000
$\text{Biotite_wOH} + \text{Eu}^{3+} + 2\text{H}_2\text{O} \leftrightarrow \text{Biotite_wOEu}(\text{OH})_2 + 3\text{H}^+$	-18.40
$\text{Quartz_sOH} + \text{Eu}^{3+} \leftrightarrow \text{Quartz_sOEu}^{2+} + \text{H}^+$	-10.69
$\text{Quartz_sOH} + \text{Eu}^{3+} + 2\text{H}_2\text{O} \leftrightarrow \text{Quartz_sOEu}(\text{OH})_2 + 3\text{H}^+$	-20.00

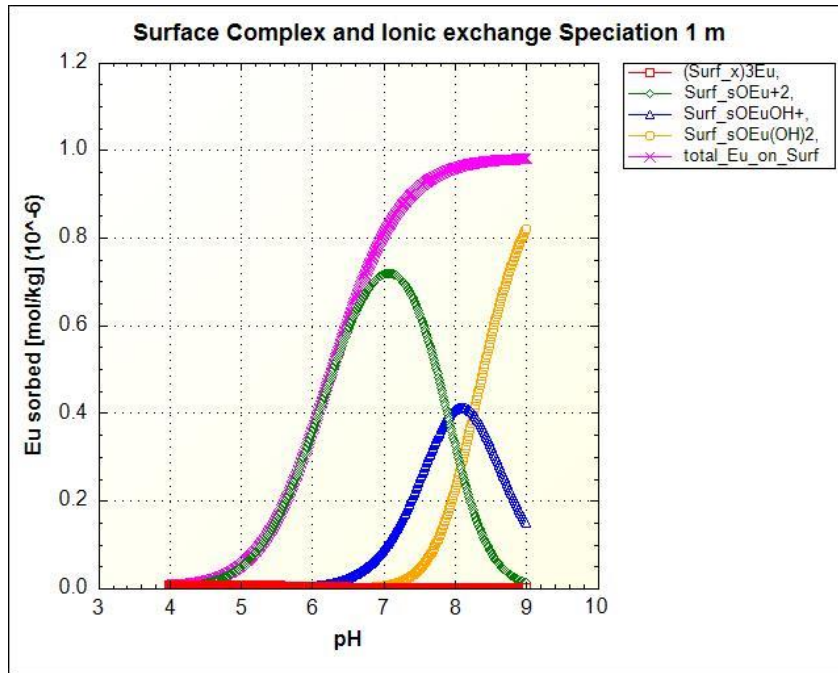
Table 10 presents the main chemical reactions identified for the optimized curve fitting. This result helps identify the mechanism for the sorption of Eu onto granite that can explain the experimental data.

Table 10: The main reactions identified for the sorption of Eu onto granite.

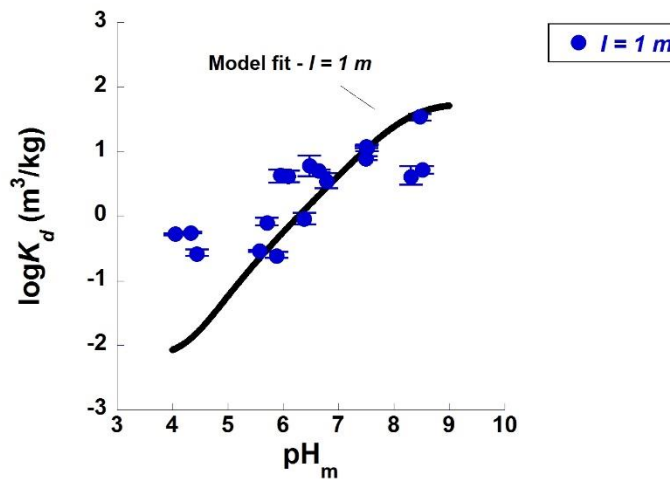
Surface complexation and Ionic exchange reactions	<i>Log_K</i>
$3\text{Surf_xNa} + \text{Eu}^{3+} \leftrightarrow (\text{Surf_x})_3\text{Eu} + 3\text{Na}^+$	7.85
$2\text{Surf_xNa} + \text{Ca}^{2+} \leftrightarrow (\text{Surf_x})_2\text{Ca} + 2\text{Na}^+$	3.18
$\text{Feldspar_sOH} + \text{Eu}^{3+} \leftrightarrow \text{Feldspar_sOEu}^{2+} + \text{H}^+$	-0.300
$\text{Feldspar_sOH} + \text{Eu}^{3+} + \text{H}_2\text{O} \leftrightarrow \text{Feldspar_sOEu}(\text{OH})^+ + 2\text{H}^+$	-8.70
$\text{Biotite_sOH} + \text{Eu}^{3+} \leftrightarrow \text{Biotite_sOEu}^{2+} + \text{H}^+$	0.350
$\text{Biotite_sOH} + \text{Eu}^{3+} + \text{H}_2\text{O} \leftrightarrow \text{Biotite_sOEu}(\text{OH})^+ + 2\text{H}^+$	7.12
$\text{Biotite_sOH} + \text{Eu}^{3+} + 2\text{H}_2\text{O} \leftrightarrow \text{Biotite_sOEu}(\text{OH})_2 + 3\text{H}^+$	-15.1

5.3.2 Modeling results for Eu sorption onto MX-80 bentonite

Figure 21-25 demonstrate the modeling for Eu sorption onto MX-80 bentonite. Similarly, the surface complex species are presented together with the curve fitting.

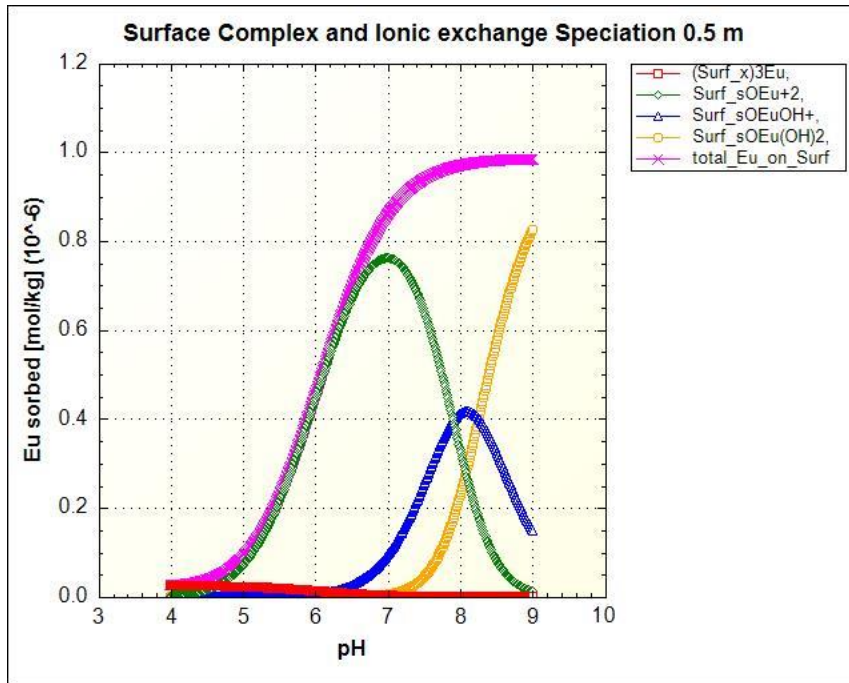


(a)

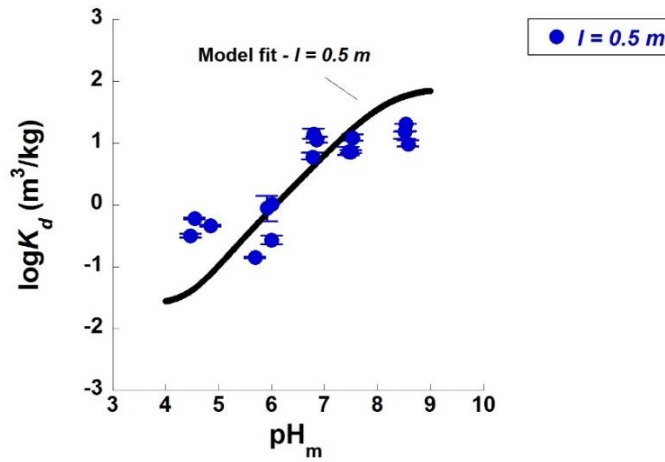


(b)

Figure 21: The sorption modeling for the sorption of Eu onto MX-80 bentonite in 1 m Ca-Na-Cl solution. (a) is the speciation of the surface complex; (b) is the curve fitting for the experimental results.

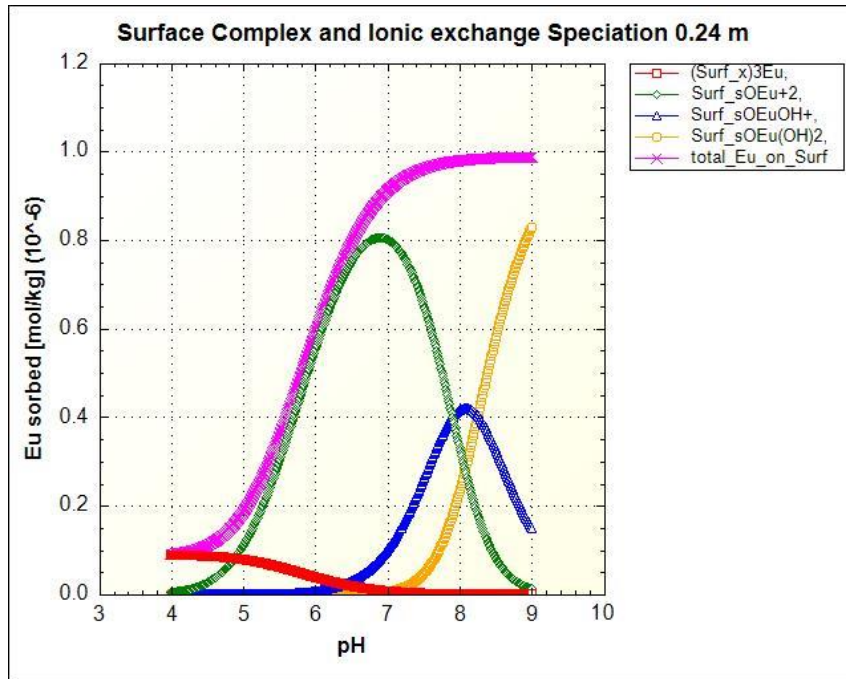


(a)

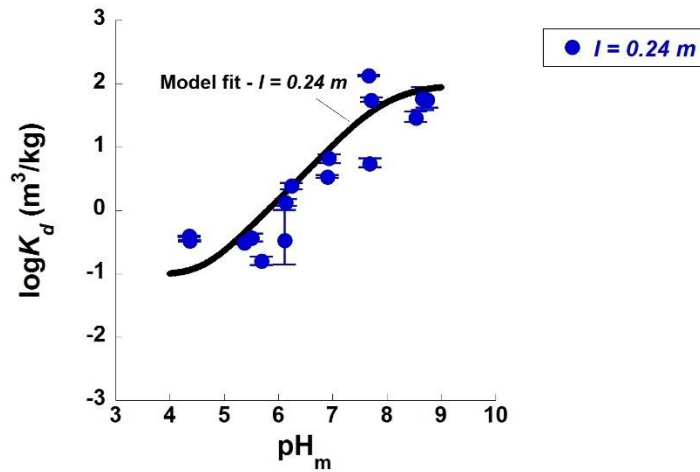


(b)

Figure 22: The sorption modeling for the sorption of Eu onto MX-80 bentonite in 0.5 m Ca-Na-Cl solution. (a) is the speciation of the surface complex; (b) is the curve fitting for the experimental results.

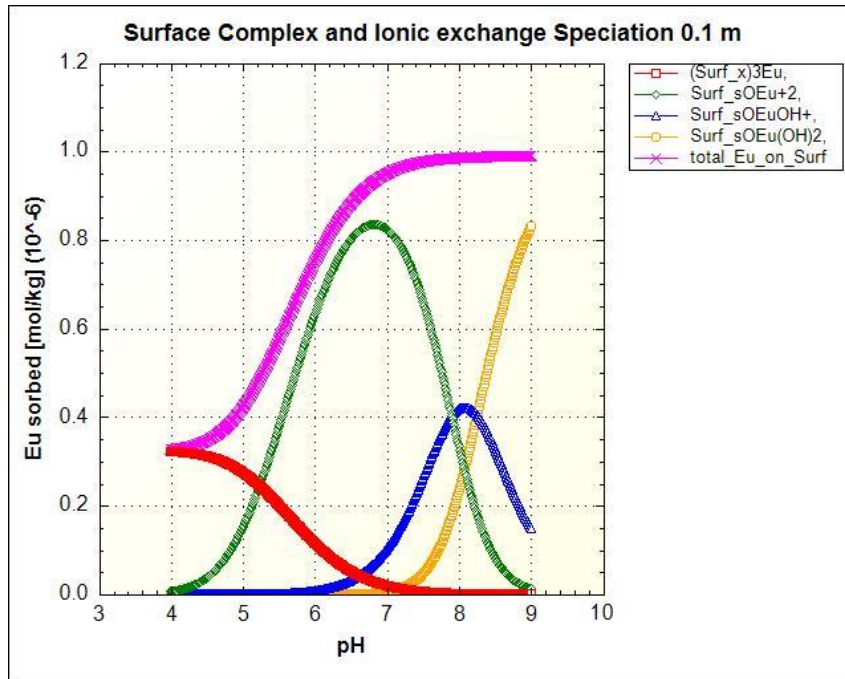


(a)

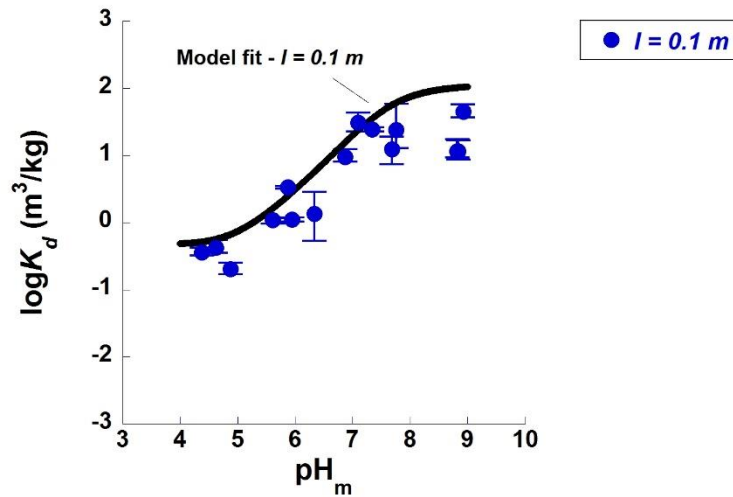


(b)

Figure 23: The sorption modeling for the sorption of Eu onto MX-80 bentonite in 0.24 m Ca-Na-Cl solution. (a) is the speciation of the surface complex; (b) is the curve fitting for the experimental results.

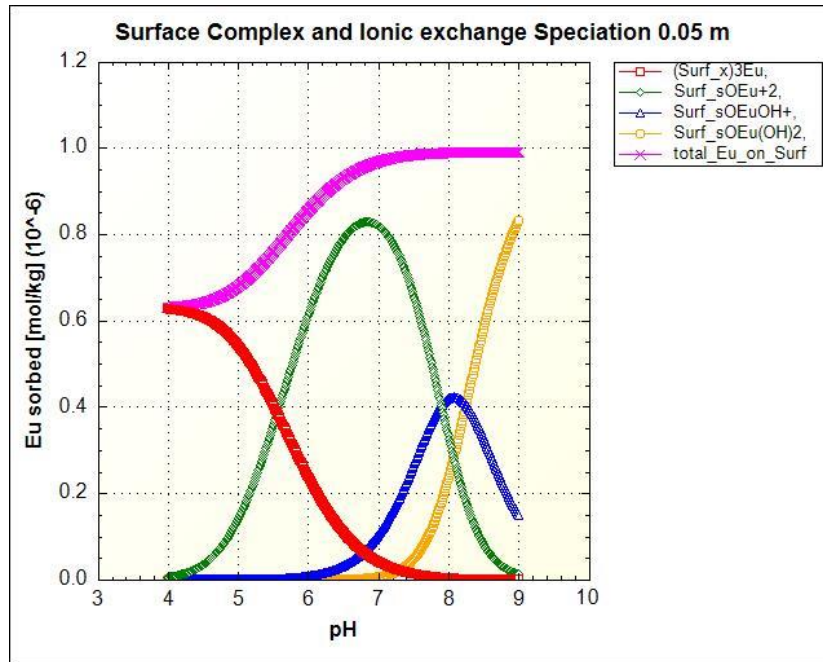


(a)

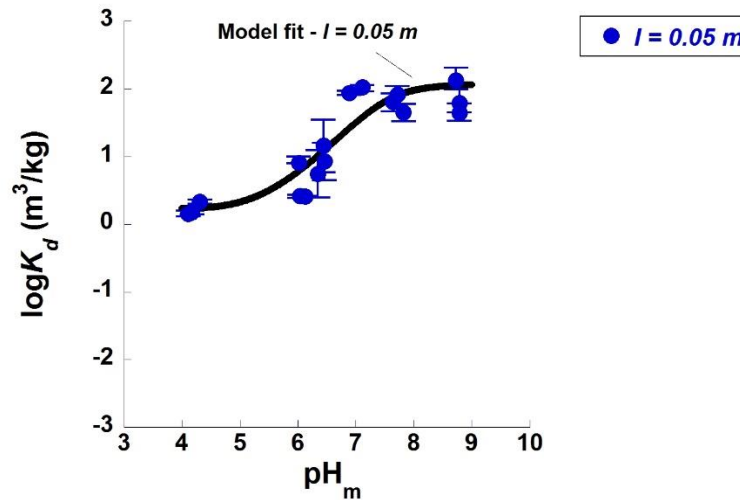


(b)

Figure 24: The sorption modeling for the sorption of Eu onto MX-80 bentonite in 0.1 m Ca-Na-Cl solution. (a) is the speciation of the surface complex; (b) is the curve fitting for the experimental results.



(a)



(b)

Figure 25: The sorption modeling for the sorption of Eu onto MX-80 bentonite in 0.05 m Ca-Na-Cl solution. (a) is the speciation of the surface complex; (b) is the curve fitting for the experimental results.

In general, the modeling result matches well with most the experimental data and follows the similar trend. There also exist some discrepancies that model underestimated the results at pH4 in 0.5 m and 1 m solutions and overestimated the results at around pH9 in 0.5 m solution. The underestimation might be attributed to the existence of EuCl_2 species, similar to the sorption onto granite. Further work is also needed to examine the effects of EuCl_2 species on the sorption of Eu onto MX-bentonite. As for the overestimation, the possible reason could be the uncertainty of the modeling itself. Since these chemical reactions are set for all ionic strength conditions, it is possible that the discrepancy occurs. In the further work, other methods such as density functional theory (DFT) could be used to examine the species and help verify the experimental results.

Similar to Eu sorption onto granite, the surface complex speciation verifies that the dominant reaction could be ionic exchange reaction at lower pH region while the surface complexation reactions dominate starting from around pH5. Based on the optimized curve fitting, Table 11 demonstrates the chemical reactions identified that could well explain the experimental data for the sorption of Eu onto MX-80 bentonite. This suggests the sorption mechanism of Eu sorption onto MX-80 bentonite. Also, the identified reactions are mainly in the form of metal coordination. This suggests that the inner-sphere complex is formed and dominates.

Table 11: The surface complexation and ionic exchange reactions with their constants from the optimized model.

Reactions	logK
$\text{Surf_xNa} + \text{H}^+ \leftrightarrow \text{Surf_xH} + \text{Na}^+$	1.20
$2\text{Surf_xNa} + \text{Ca}^{2+} \leftrightarrow (\text{Surf_x})_2\text{Ca} + 2\text{Na}^+$	3.60
$3\text{Surf_xNa} + \text{Eu}^{3+} \leftrightarrow (\text{Surf_x})_3\text{Eu} + 3\text{Na}^+$	6.55
$\text{Surf_sOH} + \text{Eu}^{3+} \leftrightarrow \text{Surf_sOEu}^{2+} + \text{H}^+$	1.15
$\text{Surf_sOH} + \text{Eu}^{3+} + \text{H}_2\text{O} \leftrightarrow \text{Surf_sOEuOH}^+ + 2\text{H}^+$	-6.75
$\text{Surf_sOH} + \text{Eu}^{3+} + 2\text{H}_2\text{O} \leftrightarrow \text{Surf_sOEu}(\text{OH})_2 + 3\text{H}^+$	-15.0

In surface chemistry, it is commonly believed that there exists a relationship between the free energies of formation of metal complexes and thermodynamic properties of the metal ions or ligands (Bradbury & Baeyens, 2005). This tendency is usually referred as linear free energy relationships (LEFRs). (Bradbury & Baeyens, 2005) proposed two equations that could well describe the correlation between the logarithm of reaction constant K_d on montmorillonite and the logarithm of the aqueous hydrolysis constants. Equations (5.3) and (5.4) present the equation relation for sorption on strong site and weak site, respectively.

Strong site:

$$\log^s K_{x-1} = 8.1 \pm 0.3 + (0.90 \pm 0.02)\log^{\text{OH}} K_x \quad (5.3)$$

Weak site:

$$\log^{W1}K_{x-1} = 6.2 \pm 0.8 + (0.98 \pm 0.09)\log^{OH}K_x \quad (5.4)$$

Where $\log^S K_{x-1}$ is the reaction constant for reactions on the strong site, $\log^{W1} K_{x-1}$ is the reaction constant for reactions on the weak site, $\log^{OH} K_x$ is the reaction constant for related aqueous species, and x is an integer (Bradbury & Baeyens, 2005).

In this work, the montmorillonite is used in the modeling of Eu sorption onto MX-80 bentonite. The chemical reactions obtained from the optimized modeling showed that the sorption mainly occurred at the strong site among the surface complexation reactions, as shown in the Table 11. The equation of LEFR can then be used as a reference criterion to check the reaction constants $\log K$ obtained from this work.

Table 12 below presents the hydrolysis constants ($\log^{OH} K_x$) for related aqueous species from JAEA database.

Table 12: The hydrolysis constants ($\log^{OH} K_x$) for related aqueous species referenced from JAEA database (Kitamura et al., 2014).

Hydrolysis reactions	$\log^{OH} K_x$
$\text{Eu}^{3+} + \text{H}_2\text{O} \leftrightarrow \text{Eu}(\text{OH})^{2+} + \text{H}^+$	-7.801
$\text{Eu}^{3+} + 2\text{H}_2\text{O} \leftrightarrow \text{Eu}(\text{OH})_2^+ + 2\text{H}^+$	-16.402
$\text{Eu}^{3+} + 3\text{H}_2\text{O} \leftrightarrow \text{Eu}(\text{OH})_3 + 3\text{H}^+$	-25.203

Here, EuOH^{2+} corresponds to Surf_sOEu^{2+} complex, Eu(OH)_2^+ refers to Surf_sOEuOH^+ complex, and Eu(OH)_3 corresponds to Surf_sOEu(OH)_2 complex (Bradbury & Baeyens, 2005).

Plug the $\log^{\text{OH}}K_x$ accordingly into the equation for strong site, it can be found that for Surf_sOEu^{2+} , the reaction constant range is $0.623 \leq \log K \leq 1.535$, while the obtained $\log K$ from this work is 1.150 which is within the range. For Surf_sOEuOH^+ , the constant range is $-7.290 \leq \log K \leq -6.034$, while the obtained $\log K$ is -6.750, which is within the range. For Surf_sOEu(OH)_2 , the constant range is $-15.387 \leq \log K \leq -13.779$, while the obtained $\log K$ is -15.000, which is also within the range.

Therefore, the reaction constants of the surface complexation obtained from the modeling agree with the LEFRs proposed in (Bradbury & Baeyens, 2005), indicating that the reaction constants obtained in this work are within a reasonable range.

6 Future work

For the next step, firstly, the sorption of Eu onto the sedimentary geological conditions including illite, shale, and limestone should be studied as a function of pH and ionic strength. The mechanism for each condition should also be examined. This is helpful for the safety assessment calculation for a deep geological repository.

Besides, as the curve fitting of the modeling suggests that the sorption results tend to reach a plateau starting from pH 9, the sorption experiments of Eu could be conducted at pH 10 to further verify. Also, as discussed in the results section, the existence of EuCl_2 might affect the sorption results, so the effects of EuCl_2 should be considered and discussed in the next step.

In this work, the surface complexes and sorption mechanisms were identified using PHREEQC modeling, mainly by fitting the experimental data to obtain the optimized reactions with their reaction constants. Other methods such as density functional theory (DFT) could be utilized in the future to help verify the surface complexes and further examine the sorption mechanism.

7 Conclusion

This study systematically investigated the effects of pH and ionic strength of Ca-Na-Cl solutions on the sorption of Eu onto granite and MX-80 bentonite over a wide range, using both sorption experimental measurements and sorption modeling. The solution conditions, granite (a crystalline rock) and MX-80 (backfill material) being used in the sorption study, are of interest to the geological disposal of used nuclear fuel.

The upper concentration limit for Eu in Ca-Na-Cl solution was found to be around 8×10^{-6} mol/L for all ionic strength. Combining with available detection limit of Eu by ICPMS, the experimental concentration was set to be 10^{-6} mol/L.

From the experimental result, the sorption on both granite and MX-80 bentonite was found to be strongly dependent on pH, whereas the ionic strength mainly exhibits effects on the sorption at lower pH region ($\text{pH} < 6$). The dependence on pH indicates that the dominating mechanism could be the surface complexation at higher pH region. The ionic strength effect at lower pH region suggests that the ionic exchange reactions are dominating as surface mainly contain $\text{S} - \text{OH}_2^+$ over the same pH region and little coordination reactions can happen. The obtained sorption coefficient K_d values can be used for the safety assessment calculation of a deep geological repository for used nuclear fuel.

The sorption modeling in PHREEQC helped identify the sorption mechanism for both granite and MX-80 bentonite. The surface complex speciation verified that the ionic

exchange reactions mainly occur at $\text{pH} < 6$, while the dominating mechanism is surface complexation at higher pH region. It also shows that ionic exchange reactions largely occur at low ionic strength such as $I = 0.05 \text{ m}$ and 0.1 m , which agrees with the theory that as the salt concentration increases, the cations compete with the interested element. At lower pH region, the model considered and identified the effects of Ca^{2+} as it competes with Eu^{3+} on the ionic exchange reaction, as this solution type is particular in the DGR groundwater condition. For both granite and MX-80 bentonite, the optimized modeling identified the possible sorption mechanisms, which could well explain the experimental data. It suggests that the mainly formed complexes of the Eu sorption might be inner-sphere complexes. For granite, the surface complex speciation in the modeling suggests that biotite might be the main affinity for Eu sorption onto granite.

8 Bibliography

- Bezzina, J. P., Neumann, J., Brendler, V., & Schmidt, M. (2022). Combining batch experiments and spectroscopy for realistic surface complexation modelling of the sorption of americium, curium, and europium onto muscovite. *Water Research*, 223, 119032.
- Bradbury, M. H., & Baeyens, B. (2002). Sorption of Eu on Na- and Ca-montmorillonites: Experimental investigations and modelling with cation exchange and surface complexation. *Geochimica et Cosmochimica Acta*, 66(13), 2325–2334.
- Bradbury, M. H., & Baeyens, B. (2005). Modelling the sorption of Mn(II), Co(II), Ni(II), Zn(II), Cd(II), Eu(III), Am(III), Sn(IV), Th(IV), Np(V) and U(VI) on montmorillonite: Linear free energy relationships and estimates of surface binding constants for some selected heavy metals and actinides. *Geochimica et Cosmochimica Acta*, 69(4), 875–892.
- Brandani, S. (2021). Kinetics of liquid phase batch adsorption experiments. *Adsorption*, 27(3), 353–368.
- Davis, J. A., & Kent, D. B. (2018). CHAPTER 5. SURFACE COMPLEXATION MODELING IN AQUEOUS GEOCHEMISTRY. In *CHAPTER 5. SURFACE*

COMPLEXATION MODELING IN AQUEOUS GEOCHEMISTRY (pp. 177–260).

De Gruyter.

- Fan, Q., Li, P., Zheng, Z., Wu, W., & Liu, C. (2014). Insights into sorption species of Eu(III) on γ -Al₂O₃ and bentonite under different pH: Studies at macro- and micro-scales. *Journal of Radioanalytical and Nuclear Chemistry*, 299(3), 1767–1775.
- Fernandes, M. M., Baeyens, B., & Bradbury, M. H. (2008). The influence of carbonate complexation on lanthanide/actinide sorption on montmorillonite. *Radiochimica Acta*, 96(9–11), 691–697.
- Fukushi, K., Hasegawa, Y., Maeda, K., Aoi, Y., Tamura, A., Arai, S., Yamamoto, Y., Aosai, D., & Mizuno, T. (2013). Sorption of Eu(III) on Granite: EPMA, LA-ICP-MS, Batch and Modeling Studies. *Environmental Science & Technology*, 47(22), 12811–12818.
- Grambow, B., Fattahi, M., Montavon, G., Moisan, C., & Giffaut, E. (2006). Sorption of Cs, Ni, Pb, Eu(III), Am(III), Cm, Ac(III), Tc(IV), Th, Zr, and U(IV) on MX 80 bentonite: An experimental approach to assess model uncertainty. *Radiochimica Acta*, 94(9–11), 627–636.
- Guo, N., Yang, J. W., Zhang, R., Ye, Y. L., Wu, W. S., & Guo, Z. J. (2015). Effects of organic acids on Eu(III) sorption on Na-bentonite. *Journal of Radioanalytical and Nuclear Chemistry*, 303(3), 2185–2192.

- Guo, Z., Xu, J., Shi, K., Tang, Y., Wu, W., & Tao, Z. (2009). Eu(III) adsorption/desorption on Na-bentonite: Experimental and modeling studies. *Colloids and Surfaces A: Physicochemical and Engineering Aspects*, 339(1), 126–133.
- He, Y., Chen, Y., Ye, W., & Zhang, X. (2020). Effects of contact time, pH, and temperature on Eu(III) sorption onto MX-80 bentonite. *Chemical Physics*, 534, 110742.
- Hurel, C., & Marmier, N. (2010). Sorption of europium on a MX-80 bentonite sample: Experimental and modelling results. *Journal of Radioanalytical and Nuclear Chemistry*, 284(1), 225–231.
- Iida, Y., Yamaguchi, T., Tanaka, T., & Hemmi, K. (2016). Sorption behavior of thorium onto granite and its constituent minerals. *Journal of Nuclear Science and Technology*, 53(10), 1573–1584.
- Jin, Q., Wang, G., Ge, M., Chen, Z., Wu, W., & Guo, Z. (2014). The adsorption of Eu(III) and Am(III) on Beishan granite: XPS, EPMA, batch and modeling study. *Applied Geochemistry*, 47, 17–24.
- Karimzadeh, L., Lippold, H., Stockmann, M., & Fischer, C. (2020). Effect of DTPA on europium sorption onto quartz – Batch sorption experiments and surface complexation modeling. *Chemosphere*, 239, 124771.
- Kitamura, A., Doi, R., & Yoshida, Y. (2014). Update of JAEA-TDB. Update of thermodynamic data for palladium and tin, refinement of thermodynamic data for protactinium, and preparation of PHREEQC database for use of the Brønsted-Guggenheim-Scatchard model. *Japan Atomic Energy Agency*.

- Kumar, S., Godbole, S. V., & Tomar, B. S. (2013). Speciation of Am(III)/Eu(III) sorbed on γ -alumina: Effect of metal ion concentration. *Radiochimica Acta*, 101(2), 73–80.
- Lee, S.-G., Lee, K. Y., Cho, S. Y., Yoon, Y. Y., & Kim, Y. (2006). Sorption properties of ^{152}Eu and ^{241}Am in geological materials: Eu as an analogue for monitoring the Am behaviour in heterogeneous geological environments. *Geosciences Journal*, 10(2), 103–114.
- Li, H., He, B., Li, P., Fan, Q., Wu, H., Liang, J., Liu, C., & Yu, T. (2019). Adsorption behaviors of Eu(III) on granite: Batch, electron probe micro-analysis and modeling studies. *Environmental Earth Sciences*, 78(8), 249.
- Li, P., Wu, H., Liang, J., Yin, Z., Pan, D., Fan, Q., Xu, D., & Wu, W. (2017). Sorption of Eu(III) at feldspar/water interface: Effects of pH, organic matter, counter ions, and temperature. *Radiochimica Acta*, 105(12), 1049–1058.
- Naserifard, N., Lee, A., Birch, K., Chiu, A., & Zhang, X. (2021). *Deep geological repository conceptual design report crystalline/sedimentary rock* (p. 187).
- Neumann, J., Brinkmann, H., Britz, S., Lützenkirchen, J., Bok, F., Stockmann, M., Brendler, V., Stumpf, T., & Schmidt, M. (2021). A comprehensive study of the sorption mechanism and thermodynamics of f-element sorption onto K-feldspar. *Journal of Colloid and Interface Science*, 591, 490–499.
- Ortiz-Oliveros, H. B., Flores Espinosa, R. M., Ávila-Pérez, P., Cruz-Gonzalez, D., & Ouerfelli, N. (2021). Prediction of Europium Retention in Perovskite: Potential

- Candidates for an Engineering Barrier in the Disposal of Radioactive Waste.
Journal of Chemistry, 2021, e3985582.
- Parkhurst, D. L., & Appelo, C. A. J. (2013). *USGS - Description of Input and Examples for PHREEQC Version 3—A Computer Program for Speciation, Batch-Reaction, One-Dimensional Transport, and Inverse Geochemical Calculations*. U.S. Geological Survey.
- Qi, W., Tian, L., Liu, B., Lin, J., Liu, D., Tu, P., Liu, P., Li, Z., Chen, X., & Wu, W. (2015). Adsorption of Eu(III) on defective magnetic FeNi/RGO composites: Effect of pH, ion strength, ions and humic acid. *Journal of Radioanalytical and Nuclear Chemistry*, 303(3), 2211–2221.
- Rabung, Th., Pierret, M. C., Bauer, A., Geckeis, H., Bradbury, M. H., & Baeyens, B. (2005). Sorption of Eu(III)/Cm(III) on Ca-montmorillonite and Na-illite. Part 1: Batch sorption and time-resolved laser fluorescence spectroscopy experiments. *Geochimica et Cosmochimica Acta*, 69(23), 5393–5402.
- Riddoch, J. (2016). SORPTION OF PALLADIUM ONTO BENTONITE, ILLITE AND SHALE UNDER HIGH IONIC STRENGTH CONDITIONS. *McMaster University, MAsc Thesis*.
- Sheng, G. D., Shao, D. D., Fan, Q. H., Xu, D., Chen, Y. X., & Wang, X. K. (2009). Effect of pH and ionic strength on sorption of Eu(III) to MX-80 bentonite: Batch and XAFS study. *Rca - Radiochimica Acta*, 97(11), 621–630.
- Spahiu, K., & Bruno, J. (1995). *A selected thermodynamic database for REE to be used in HLNW performance assessment exercises*.

- Stern, O. (1924). Zur Theorie Der Elektrolytischen Doppelschicht. *Zeitschrift Für Elektrochemie Und Angewandte Physikalische Chemie*, 30(21–22), 508–516.
- Stumm, W. (1995). *Aquatic Chemistry: Chemical Equilibria and Rates in Natural Waters*. John Wiley & Sons, Incorporated.
- Tan, X., Fan, Q., Wang, X., & Grambow, B. (2009). Eu(III) Sorption to TiO₂ (Anatase and Rutile): Batch, XPS, and EXAFS Studies. *Environmental Science & Technology*, 43(9), 3115–3121.
- Tertre, E., Berger, G., Simoni, E., Castet, S., Giffaut, E., Loubet, M., & Catalette, H. (2006). Europium retention onto clay minerals from 25 to 150°C: Experimental measurements, spectroscopic features and sorption modelling. *Geochimica et Cosmochimica Acta*, 70(18), 4563–4578.
- Vilks, P., & Yang, T. (2018). Sorption of Selected Radionuclides on Sedimentary Rocks in Saline Conditions – Updated Sorption Values. *NWMO-TR-2018-03*.
- Wang, X., Sun, Y., Alsaedi, A., Hayat, T., & Wang, X. (2015). Interaction mechanism of Eu(III) with MX-80 bentonite studied by batch, TRLFS and kinetic desorption techniques. *Chemical Engineering Journal*, 264, 570–576.
- Yang, J., Racette, J., Garcia, F. G., Nagasaki, S., & Yang, T. (2022). Sorption of Eu on MX-80 Bentonite in Na–Ca–Cl Brine Solutions. *Journal of Nuclear Fuel Cycle and Waste Technology(JNFCWT)*, 20(2), 151–160.
- Zavarin, M., Roberts, S. K., Hakem, N., Sawvel, A. M., & Kersting, A. B. (2005). Eu(III), Sm(III), Np(V), Pu(V), and Pu(IV) sorption to calcite. *Radiochimica Acta*, 93(2), 93–102.

Zhang, H., He, H., Liu, J., Li, H., Zhao, S., Jia, M., Yang, J., Liu, N., Yang, Y., & Liao, J. (2021). Sorption behavior of Eu(III) on Tamusu clay under strong ionic strength: Batch experiments and BSE/EDS analysis. *Nuclear Engineering and Technology*, 53(1), 164–171.